MECHANICAL PROPERTIES OF GLASS FIBER REINFORCED CONCRETE AND APPLICATIONS IN STRUCTURAL DESIGN

by

Bakul B. Desai

B.E., L.D. College of Engineering
Gujarat University, 1977
India

A MASTER'S REPORT

submitted in partial fulfillment of

the requirements for the degree

MASTER OF SCIENCE

Department of Civil Engineering

KANSAS STATE UNIVERSITY
Manhattan, Kansas

1980

Approved:

Major Professor

TABLE OF CONTENTS

TABLE OF CONTENTS (continued)

LIST OF FIGURES

LIST OF FIGURES (continued)

LIST OF TABLES

Mechanical Properties of Glass Fiber Reinforced Concrete and Applications in Structural Design

Chapter 1

INTRODUCTION

1.1 History

Fiber reinforcement of cement and concrete is not really a new concept. Even in an ancient time the use of straw in bricks and horse's hair in mortar indicates a direction toward fiber reinforcement. Nature, too, has provided man with fiber reinforced construction materials in the form of bamboo and wood.

1.2 Development

One of the problems of a cement based matrix is the inherently brittle type of failure under the influence of tensile stress systems or dynamic loadings. Only two to five percent by volume of fiber addition to concrete leads toward an achievement of altering and improving the useful material properties like fatigue resistance, fracture toughness and flexural strength (4). The higher modulus of elasticity fibers will provide the primary stiffening action before the matrix cracks. After cracking of the matrix, assuming the bond is good, fibers will continue to carry the load, depending on their ductility.

The fibers that are currently being investigated as reinforcement for concrete include steel (stainless and carbon), alkali-resistant glass and polypropylene. Other types such as polythylene, E glass, nylon and rayon have been suggested in the past, but factors like high cost, low effectiveness or high susceptibility to the alkali attack from the cement environment ruled them out of consideration (1).

This report deals with only glass fibers as the reinforcement of concrete. The potential of using glass fiber reinforced cement (GRC) was recognized first by the Russians in 1941 (3) when they developed a technique of using glass fibers as a reinforcing material. Primary experimental work was confined only to the high alumina cement because of the fact that glass fibers are unable to withstand high alkalinity generated in the portland cement environment.

The doors of further development were opened when Dr. A. J. Majumdar of the Building Research Establishment in England conceived a glass composition which had a far greater alkalinity resistance (3). Pilkington Brothers Limited of England has patented this new range of glass fibers under the name 'CEM-FIL'. With this the difficulties met with other glass fibers may greatly be overcome. The use of such fibers in reinforcement of concrete gives us a major advantage, namely an increase in long term impact resistance. Subsequently, the work to failure as measured by the area under the load/deflection curve to the point of failure is magnified 4 to 5 times with the addition of about three percent of fiber by weight to the concrete (10). However, extensive research is still in progress to find an access to heavy structural applications of glass fiber reinforced concrete.

This report will cover primarily the mechanical properties of glass fiber reinforced concrete obtained from experimental data, the theories of fiber reinforcement and their applications to structural analysis, and major advantages and potential limitations of glass fiber reinforced concrete.

Chapter 2

GENERAL

2.1 Definition of Glass Fiber Reinforced Composite (GRC)

GRC may be defined as a composite material made up of a matrix of cement with other fine aggregates like sand, pulverized fuel ash, limestone dust or inert material filler and water, reinforced with glass fibers.

2.2 Material Properties

2.2.1 Properties of fibers - The theoretical behavior of the composite material is greatly characterized by the physical properties of fibers and the matrix and bond strength between the two. Typical physical properties of various fibers are tabulated in Table 2-1 (1).

The fiber types shown in Table 2-1 can be separated into two categories, one with their moduli of elasticity lower than the matrix, e.g., cellulose, polypropylene and nylon; and other with higher moduli, e.g., glass, steel, carbon, asbestos and Kevlar. The organic fibers with low moduli are subject to relatively high creep and hence are not suitable for a cracked composite design as they exhibit considerable elongations over a period of time. Also, their large values of Poisson's Ratio in combination with low moduli (giving high ductility), cause the fibers to stretch and pull away from the matrix, thus debonding before the fibers rupture.

Table 2-1 (1)

Typical fiber properties

Fibre	Diameter μm	Length mm	Density $Kg/m^3 10^3$	Young's Modulus GN/m^2	Poisson's Ratio	Tensile Strength MN/m^2	[a]Elongation at break %	Typical Volume in Composite
Chrysotile (white) Asbestos	0.02'-30	<40	2.55	164	0.3	200-1800 (fibre bundles)	2-3	10
Crocidolite (blue)	0.1-20	--	3.37	196	--	3,500	2-3	--
Type 1 (High modulus) Carbon	8	10-continuous	1.90	380	0.35	1,800	~0.5	2-12
Type 2 (High strength)	9		1.90	230		2,600	~1.0	
Cellulose			1.2	10		300-500		10-20
E	8-10		2.54	72	0.25	3,500	4.8	
Glass Cem-Fil filament	12.5	10-50		80	0.22	2,500	3.6	2-8
204 filament strand	110x650		2.7	70	--	1,250	--	
PRD 49	10		1.45	133	0.32	2,900	2.1	
Kevlar		6-65						<2
PRD 29	12		1.44	69	--	2,900	4.0	
Nylon (Type 242)	>4	5-50	1.14	Rate dependent up to 4	0.40	750-900	13.5	0.1-6
Monofilament	100-200	5-50	0.9	Rate dependent up to 5	--	400	18	0.1-6
Polypropylene					0.29-			
Fibrillated	500-4000	20-75	0.9	up to 8	0.46	400	8	0.2-1.2
High tensile	100-600			200		700-2000	3.5	
Steel		10-60	7.86		0.28			0.5-2
Stainless	10-330			160		2,100	3	

[a]Note: one percent elongation = $10,000 \times 10^{-6}$ strain.

Table 2-2 (10)

Chemical composition of some glasses available as fiber (weight percent)

	E-glass	A-glass	Alkali-resistant glass
SiO_2	52.4	72.2	71
K_2O Na_2O }	0.8	13.0	11
B_2O_3	10.4	--	--
Al_2O_3	14.4	1.8	1
MgO	5.2	3.5	--
CaO	16.6	9.5	--
ZrO_2	--	--	16
Li_2O	--	--	1

Various glasses are available as fibers. Table 2-2 (10) gives an idea about the chemical composition of these glasses. The glass fibers are available in the forms of glasswool, glass roving, or chopped glass strands. The chopped strand mat is suitable to achieve a directional reinforcement advantage; i.e., concentration of glass fiber reinforcement in a particular plane.

Table 2-3 (10)

Properties of single filaments of glass

	E-glass	A-glass	Alkali-resistant glass
Density (g/cm^3)	2.54	2.46	2.78
Tensile strength (MN/m^2)	3500	3100	2500
Modulus of elasticity (GN/m^2)	72.5	65	70
Extension at break (%)	4.8	4.7	3.6

Properties of single filaments of glass are shown in Table 2-3 (10).

2.2.2 Properties of matrix - Some important properties of various matrices are as given in Table 2-4 (1). The different degrees of alkalinity associated with different matrices greatly influences the composite material's performance. The maximum particle size is also important as it governs the fiber distribution as well as fiber content. The maximum aggregate size should not exceed 20 mm. (and preferably 10 mm.) for the concrete intended to be used along with fibers. Undesirable qualities like shrinkage and surface crazing may be avoided by using at least 50 percent by volume of inert mineral filler. The free water/cement ratio also influences the strength of the matrix.

Table 2-4 (1)

Typical properties of matrix

Matrix	Density Kg/m^3	Youngs Modulus GN/m^2	Tensile Strength MN/m^2	Strain at failure $\times 10^{-6}$ m/m
Ordinary Portland Cement Paste	2,000-2,200	10-25	3-6	100-500
High Alumina Cement Paste	2,100-2,300	10-25	3-7	100-500
O.P.C. Mortar	2,200-2,300	25-35	2-4	50-150
O.P.C. Concrete	2,300-2,450	30-40	1-4	50-150

From Table 2-1 and Table 2-4 one can easily visualize that the elongations at break associated with the fibers are much larger than the failure strains of the matrix. This fact leads us to the conclusion that the matrix will crack long before the fiber strength is reached. The theoretical

post-cracking performance can be explained by this conclusion. The modulus of the composite is not much different from that of the matrix.

The values of fiber density have considerable influence on the fiber volume required theoretically. Practically, fiber weight (W_f') is generally expressed as a proportion of the weight of cement or concrete matrix. But in a theoretical treatment fiber weight (W_f) and fiber volume (V_f) are often expressed as proportions of the whole composite weight or volume as may be applicable.

Practically,

$$W_f' = \frac{\text{weight of fiber}}{\text{weight of matrix}} \times 100 \text{ percent}$$

$$= \frac{V_f D_f}{V_m D_m} \times 100 \text{ percent} \quad \text{---------- (2-1)}$$

Theoretically,

$$W_f = \frac{\text{weight of fiber}}{\text{weight of matrix + weight of fiber}} \times 100 \text{ percent}$$

$$= \frac{V_f D_f}{V_m D_m + V_f D_f} \times 100 \text{ percent} \quad \text{---------- (2-2)}$$

where

W_f = weight of fibers as a percentage of total composite weight.

W_f' = weight of fibers as a percentage of weight of matrix.

The letters V and D refer to volume and density, respectively, whereas the subscripts f and m refer to fiber and matrix, respectively.

2.3 Manufacture of Glass Fiber Reinforced Composite (GRC)

The selection of an appropriate manufacturing process has a great influence over the final properties of composite products, as the orientation of the fibers relative to the future direction of applied stress is controlled by the procedure adopted. The mixing and compaction techniques equally contribute to the properties of composites. The various fabrication methods are briefly discussed as follows.

2.3.1 Premixing - In this process all the constituents including short glass fiber strands are mixed thoroughly and the product may further be processed. This process may include casting in open molds, extrusion, pumping into closed molds or pressing. The fibers here are three dimensionally randomly oriented. Care is taken to avoid the interwining of fibers. The dispersion of fibers in water containing a thickening additive such as polythylene oxide or methyl cellulose (0.1 percent to 1 percent of total mix water) before adding the solids and mixing in a cumflow type of mixer is preferable (1). Fiber contents would vary between 2 percent and 5 percent by weight of the other dry materials. The length of the chopped strength is about 25 mm. The method of hand tamping in 25 mm layers along with mould vibration is effective. The major production methods of composite products from premixed material are briefly discussed below.

2.3.2 Gravity molding (1) - Here the casting process is identical to the normal precast concrete. Thin sections are produced quite effectively. The external mold vibration technique produces flow satisfactorily.

2.3.3 Pressing (1) - Using 1.7 percent to 2.5 percent (by weight of dry solids) of glass fibers with length varying from 11 mm. to 22 mm., flat sheets having thicknesses in the range of 10 mm. to 20 mm. can be produced with a premix pressure between 0.15 MN/m^2 and 10 MN/m^2. A water thickening admixture is required to prevent water expulsion before the fibrous mix fills the mold uniformly.

2.3.4 Injection molding (1) - Premix with a thickening admixture and up to 5 percent glass fiber content can be pumped into closed moulds. Fiber damage possibilities are associated with this process, but fence posts, window frames or hollow columns may be cast. Enough care should be taken to avoid small blowholes on the surface. Vibration can be used to assist the flow of the material.

2.3.5 Spray-up process (3) - In this process a specially designed handheld gun is used which sprays a cement slurry onto the form and chops a continuous glass roving into desired lengths at the same time. The fibers, here, are sprayed at random in the plane of the surface. The slurry delivery rate and the glass delivery rate are adjustible. Strict quality control is essential which includes,

(1) Frequent checking of material delivery rates

(2) Checking of product thickness to avoid presence of "thin spots;

(3) Periodical cutting of coupons or test boards for strength testing purpose.

For a huge product volume the spray-up process can be automated. The simplest auto spray-dewatering plant would cost around $70,000, but that provides maximum material density.

2.3.6 Other processes (3) - Although production processes based on the spray method are almost universally used, other methods are under development. In the United States, Maso Therm Corporation of Bridgeport, Connecticut has developed a continuous process for the fabrication of GRC pannels. Amey Roadstone Corporation in England has developed a centrifugal spinning process for the manufacture of GRC pipes. At the moment all the technical experimental work relates to the spray-up process.

Chapter 3

THEORIES OF FIBER REINFORCEMENT

(A) PRINCIPLES OF FIBER REINFORCEMENT IN UNIAXIAL TENSION

3.1 General

The approach to the theoretical treatment of fiber cements and concretes requires some special considerations because of the low volume of fibers and the relatively high stiffness of the matrix which subsequently imparts an improvement in ductility after cracking.

Before we start to study the behavior of fiber cements, let us have a glance at several limiting factors which we have to consider while dealing with these materials.

(i) Low tensile failure strain ($<500 \times 10^{-6}$ m/m).

(ii) High modulus of elasticity (7-40 GN/m^2) which is useful for deflection control, but does not allow the full load carrying capacity of the fibers until cracking takes place.

(iii) Limited quantity of fibers that can be used (<10 percent by volume in cement paste).

(iv) High alkalinity of the paste (pH = 12) which causes deterioration of glass fibers.

(v) Poor bonding between fiber and matrix.

3.2 Simplified Theory for Uniaxial Tension Before Cracking

Many of the severally suggested rigorous theories cannot predict the mechanical behavior of the fiber composites accurately because of the low matrix failure strain as compared to that of fiber, low fiber volume, uneven fiber distribution, relatively poor bonding, and other time-dependent factors which get altered as hydration continues.

While discussing this theory we would refer to the ultimate strength of the matrix as the first crack strength. At this stage the cracks start to propagate just before visible cracking occurs.

3.2.1 Assumptions - To simplify the complexity in the analysis, the following assumptions are made, none of which are true in practice. (Refer to a composite shown in Fig. 3-1.)

(i) The fibers are aligned in the direction of stress.

(ii) Equal strains occur in fiber and matrix, i.e., the fibers are fully bonded before cracking.

(iii) The Poisson's ratios in fiber and matrix are zero.

3.2.2 Theory - Let A, V, E, σ, ε and F represent area, volume, Young's modulus, stress, strain and force, respectively, and let suffices f, m, c and u represent the quantities with respect to fiber, matrix, composite and ultimate stage, respectively. Consider a unit cross-sectional area of the composite i.e., $A_c = 1$ and a unit volume of composite $V_c = 1$.

The ratio of the fiber volume V_f to the composite volume V_c is

$$\frac{V_f}{V_c} = \frac{V_f}{1} .$$

Now $\varepsilon_c = \varepsilon_f = \varepsilon_m = \frac{\sigma_c}{E_c} = \frac{\sigma_f}{E_f} = \frac{\sigma_m}{E_m}$.

Hence, $\frac{\sigma_f}{\sigma_m} = \frac{E_f}{E_m} = M$ the modular ratio. ---------- (3-1)

Force $F = \sigma_c A_c$

$= \sigma_f \cdot A_f + \sigma_m \cdot A_m$.

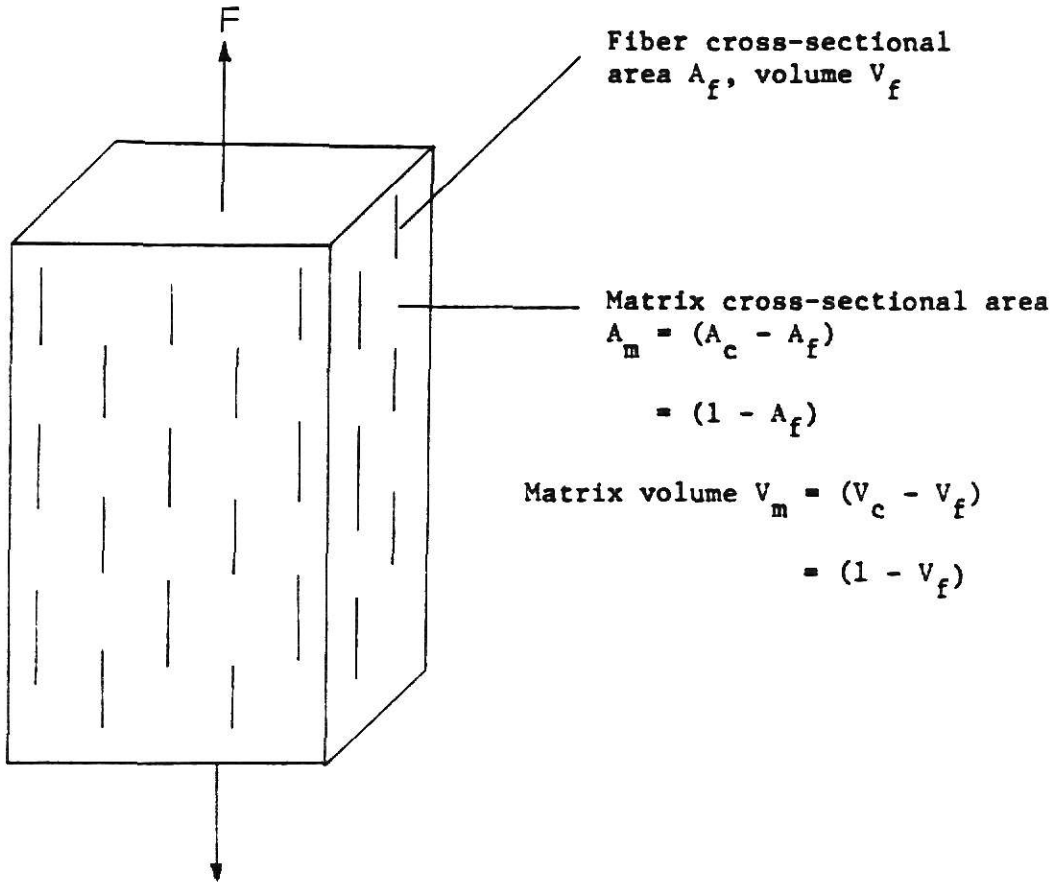

Fig. 3-1 Aligned fiber composite tested in uniaxial tension (1)

The average stress σ_c over a unit area of composite ($A_c = 1$), for a given strain ε_c before cracking is

$$\sigma_c = \sigma_f A_f + \sigma_m A_m$$

$$= \sigma_f A_f + \sigma_m (1-A_f).$$

For a unit length

$$V_c = A_c = 1 \text{ and } V_f = A_f \cdot 1 = A_f.$$

$$\sigma_c = \sigma_f V_f + \sigma_m (1-V_f). \text{ ---------- (3-2)}$$

$$\therefore \frac{\sigma_c}{\sigma_m} = \frac{\sigma_f}{\sigma_m} V_f + (1-V_f).$$

Substituting into equation (3-1)

$$\frac{\sigma_c}{\sigma_m} = MV_f + 1-V_f,$$

$$\therefore \frac{\sigma_c}{\sigma_m} = 1 + V_f (M-1), \text{ ---------- (3-3)}$$

$$\therefore \sigma_m = \frac{\sigma_c}{1 + V_f (M-1)}.$$

Now $\frac{\sigma_c}{\sigma_m} = \frac{E_c}{E_m} = 1 + V_f \left(\frac{E_f}{E_m} - 1\right)$,

$$\therefore E_c = E_f V_f + E_m (1-V_f). \text{ ---------- (3-4)}$$

Specific case of glass reinforced cement:

$$V_f = 0.05,\ E_f = 70\ GN/m^2,\ E_m = 17\ GN/m^2,$$

$$\sigma_m = \frac{\sigma_c}{1 + 0.05\ (4.12-1)} = \frac{\sigma_c}{1.16}. \text{ ---------- (3-5)}$$

From equation (3-5) it can be concluded that the 5 percent by volume addition of fiber increases the cracking stress by 16 percent as compared to the unreinforced matrix. A similar

advantage may be derived more cheaply by reducing the W/c ratio. Again for low modulus fibers the value of the cracking stress may decrease with the increase in volume of fibers. Thus, precracking performance is not greatly affected by the addition of fiber. Allen (11) has shown that even in the case of glass fibers the initial composite modulus may be less than that of the matrix alone, if the various efficiency factors given below are considered.

3.2.3 Fiber orientation - Table 3-1 (1) shows the efficiency factor n, for different types of orientations of fibers with respect to the direction of stress.

Table 3-1 (1)
Efficiency factor, n_1, for a given fiber orientation relative to the direction of stress

Fiber Orientation	n_1 given by Cox	n_1 given by Krenchel
1-D aligned	1	1
2-D random in-plane	1/3	3/8
3-D random	1/6	1/5

Here, V_f is replaced by $n_1 V_f$.

3.2.4 Fiber length - As suggested by Allen for thin composites, a second efficiency factor is required which is dependent on fiber length. Calling this factor n_2 equations (3-2) and (3-4) become

$$\sigma_c = n_1 n_2 \sigma_f V_f + \sigma_m (1-V_f)$$

$$E_c = n_1 n_2 E_f V_f + E_m (1-V_f), \text{ respectively.}$$

The factor n_2 is determined by the length of the fiber (ℓ) with relation to the critical fiber length 'ℓ_c' where ℓ_c is defined as twice the minimum length of fiber embedment which causes failure of the fiber in a pull out test. As per Allen (11),

$$\text{for } \ell \leq \ell_c \qquad n_2 = \frac{\ell}{2\ell_c}$$

$$\text{for } \ell \geq \ell_c \qquad n_2 = 1 - \frac{\ell_c}{2\ell}$$

3.3 Theory for Uniaxial Tension-Post Cracking Behavior

One of the major purposes for the inclusion of fibers as the reinforcement is that the bridging action of the fibers across the crack greatly improves the load carrying capacity of the fibers after cracking.

3.3.1 Calculations of critical fiber volume

- Critical fiber volume is defined as the volume of fibers which after matrix cracking would carry the load which the composite sustained before cracking.

Just for the sake of simplicity, let us make the same unrealistic assumptions which we made in the beginning of the chapter. Let,

ε_{mu} = matrix cracking strain,

σ_{mu} = matrix cracking stress,

$V_{f(crit)}$ = critical fiber volume,

σ_{fu} = maximum failure stress of fully bonded or pull-out stress of debonded fibers.

At the cracking stage,

$$\varepsilon_f = \varepsilon_{mu},$$

$$\sigma_f = \varepsilon_{mu} \cdot E_f,$$

$$\sigma_{mu} = \varepsilon_{mu} \cdot E_m .$$

Substituting these values in equation (3-2) just before cracking,

$$\sigma_c = \varepsilon_{mu} E_f V_{f(crit)} + \sigma_{mu} (1-V_{f(crit)}). \text{ ------- (3-6)}$$

After cracking $\sigma_{mu} = 0$ and for the condition that the same σ_c must be carried by the fiber alone;

$$V_{f(crit)} \sigma_{fu} = \varepsilon_{mu} E_f V_{f(crit)} + \sigma_{mu} (1-V_{f(crit)}).$$

-------- (3-7)

$$\therefore V_{f(crit)} = \frac{\sigma_{mu}}{(\sigma_{fu} - \varepsilon_{mu} E_f + \sigma_{mu})} . \text{ ---------- (3-8)}$$

In order to achieve economy the value of $V_{f(crit)}$ should be minimum possible. It is obvious from equation (3-8) that reduction in $V_{f(crit)}$ may be obtained from reduction in σ_{mu}, increase in σ_{fu} or reduction in ε_{mu} or E_f. For glass fiber bundles in cement paste, $V_{f(crit)}$ ≈0.4 percent (idealized).

3.4 Realistic Calculations for Critical Fiber Volume for GRC

3.4.1 Orientation effects - As mentioned before the spray-suction technique in the manufacture of GRC renders a two dimensional random in-plane distribution of fibers, and the efficiency factor for that is given as per Table 3-1 as 3/8.

3.4.2 Bond strength, fiber pull out load, fiber length - In GRC the fibers break rather than pull out. Laws (12) suggested the

length efficiency factor of $(1 - \frac{2\ell_c}{3\ell})$ for GRC where ℓ_c is defined as twice the embedded length at fiber failure. Majumdar (10) and Oakley's (13) work gave the value of ℓ_c to be 12 mm. and 26 mm. depending on age and storage conditions. Chopped glass fibers generally are 34 mm. long (ℓ = 34 mm.) and the different choices of (ℓ_c) as denoted before give the efficiency varying between 0.48 and 0.76.

Assuming $V_{f(crit)}$ = 0.4 percent for the ideal case, the critical fiber volume for a real two dimensional GRC can be approximately determined as

$$V_{f(crit)} \simeq 0.4 \frac{1}{3/8} \frac{1}{(0.76) \text{ or } (0.48)},$$

$$\simeq 1.4 \text{ percent to } 2.2 \text{ percent.}$$

3.4.3 Alternative approach - Oakley and Proctor (13) suggested an alternative way of calculating $V_{f(crit)}$ for a particular case of spray-dewatered, pseudo-random, two dimensional reinforcement with a sand/cement ratio <0.6.

Longitudinal direction:

$$\text{post cracking modulus } E_c \simeq 0.26\, E_f V_f,$$

$$\text{strength } \sigma_c \simeq 0.27\, \sigma_f V_f. \quad \text{---------- (3.9)}$$

Lateral direction:

$$E_c \simeq 0.16\, E_f V_f,$$

$$\sigma_c \simeq 0.17\, \sigma_f V_f.$$

Substituting equation (3-9) into equation (3-7) and using the respective orientation factors on the RHS,

$$0.27\ \sigma_f V_{f(crit)} = \varepsilon_{mc_u} E_f \frac{3}{8} V_{f(crit)} + \sigma_{mc_u} \left(1 - \frac{3}{8} V_{f(crit)}\right)$$

$$\therefore V_{f(crit)} = \frac{\sigma_{mc_u}}{0.27\ \sigma_f - \varepsilon_{mc_u} \frac{3}{8} E_f + \frac{3}{8} \sigma_{mc_u}} \text{ ---------- (3.10)}$$

where $\sigma_{mc_u} \simeq \sigma_{cu}$.

Using realistic values for

$\sigma_{mc} = 5 \times 10^6$ N/m^2 $\quad$ $\varepsilon_{mc} = 300 \times 10^{-6}$ m/m

$\sigma_f = 1250 \times 10^6$ N/m^2 $\quad$ $E_f = 70 \times 10^9$ N/m^2

$V_{f(crit)} \simeq 1.5$ percent

This value agrees with the one obtained before. The inclusion of 1.5 percent of fibers in GRC by the spray-suction is very easy and hence there is considerable increase in direct tensile stress, which has also been confirmed by the experiments.

(B) THEORETICAL PRINCIPLES OF FIBER REINFORCEMENT IN FLEXURE

3.5 General

Major structural components of cement bound composites are likely to be subjected to flexural stresses in addition to direct stresses. Thus, this case being more important than the case of uniaxial tension is described in detail.

The large differences between the modulus of rupture and the direct tensile strength observed experimentally made a separate theoretical treatment for flexure essential. This discrepancy results from the fact that the post-cracking stress-strain curve on the tensile side is entirely different from that on the compression side in the case of a fiber cement or concrete beam. Therefore, conventional beam theory is inapplicable (1).

Figure 3-2 (1) shows a fiber reinforced beam subjected to an increasing load P . Now as the tensile strain increases, the cracks appear. But a fraction of the load is carried by the fibers across the crack and hence equilibrium is maintained. Because of the formation of these cracks, the measured tensile strains become large and the distance to the neutral axis from the tensile surface d_n increases. On further increment of load, the tensile strains increase at a greater rate than the compressive strains because of the shift of the neutral axis. The stress blocks are as shown in Figure 3-2 (b), (c) and (d). These stress blocks are dependent of the type of composite and the load carried by the fibers across the crack.

The stress blocks (c) and (d) represent glass reinforced cement where the fiber content is very near or well above the critical fiber volume. A triangular stress block is assumed on the compression side, although that is not necessarily true at the ultimate load for fiber volumes above $V_{f(crit)}$. The load that the beam can carry in flexure can be increased by the increased area of the stress block on the tension side caused by the pseudo-ductility and an upward movement of the neutral axis. This is the reason why the values of modulus of rupture often quoted are not the real values nor do they represent tensile strengths.

3.6 The Post-cracking Flexural Behavior of Fiber Cement and Fiber Concrete Composites

Because a series of skeptical assumptions has to be made, it is very difficult to make an accurate prediction from first principles of the flexural strength of fiber composites. The assumptions made are related to fiber-fiber interaction, fiber-aggregate interaction, fiber distribution and orientation, length efficiency factors, and the bond behavior under

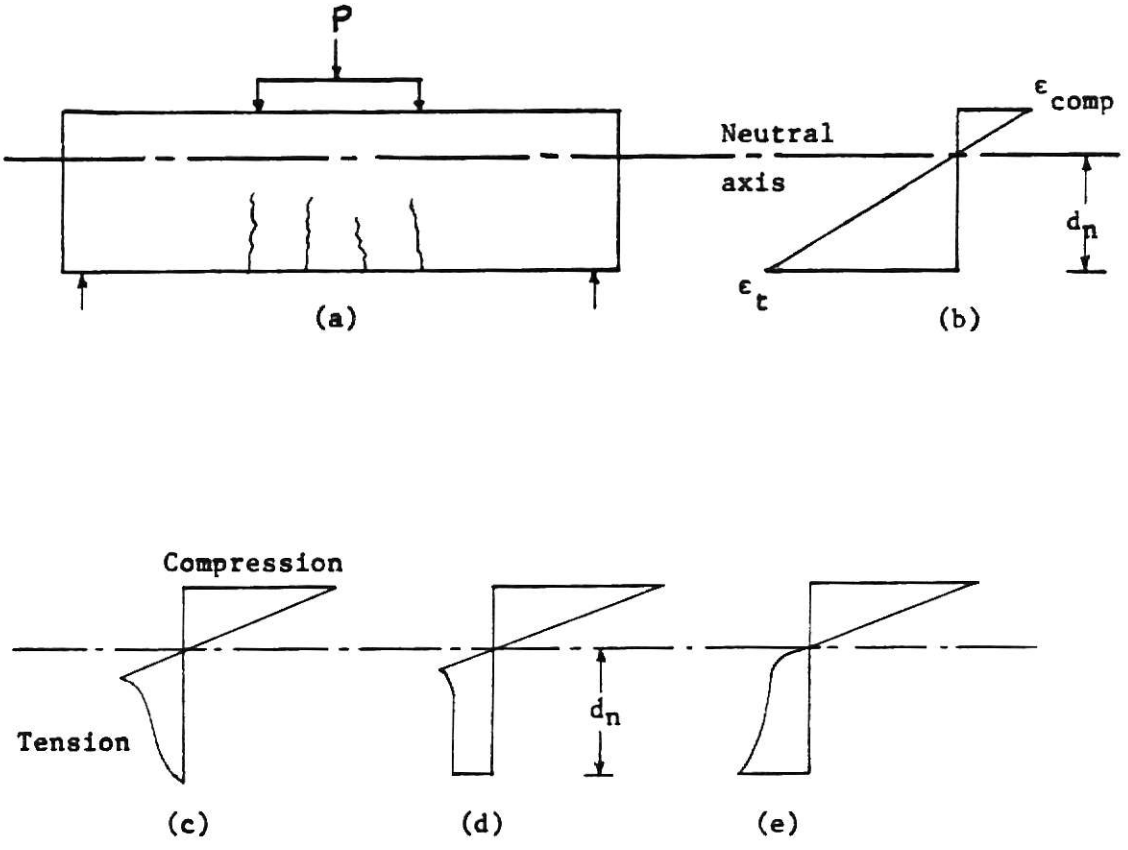

Fig. 3-2 Strain and stress distributions in cracked fiber-cement or fiber-concrete sections subjected to flexure. (a) Flexural specimen under load, (b) Average strain distribution after cracking, (c)(d)(e) Alternative stress blocks depending on type of composite and volume fraction of fibers. (1)

strain gradients. Accurate theoretical treatments have been suggested by Aveston, Sillwood and Mercer (14), derived from the theoretical prediction of the direct tensile stress-strain curve. According to their theory the modulus of rupture may be three times larger than the ultimate tensile strength in the case of fiber composites. Here the restriction is that failure must start at the tension surface.

An approximate theory has been presented by Hannant (1) in which some of the principles are the same as that of given by Aveston (14). This theory is useful in modifying the moment of resistance of a section. The modification is brought by the post-cracking ductility provided by fibers.

3.7 Analysis Using a Rectangular Stress Block in the Tensile Zone of a Beam

This analysis assumes the rectangular stress block on the tension side after cracking for simplification. This assumption is not very accurate as for all the fiber composites the shape of the stress block is influenced by fiber type, fiber volume, fiber length, crack width, curing condition and water/cement ratio. Although in many cases that may be a very close assumption.

Figure 3-3 (a) (1) represents an elastic material with the neutral axis at mid-depth and the modulus of rupture σ_{MR} equal to the tensile cracking strength of the composite σ_t. Figure 3-3 (b) shows a typical stress block for a fiber concrete composite after cracking in which the fibers are extending or are pulling out at constant load across a crack throughout the tensile zone.

According to Allen (11), for glass reinforced cement the neutral axis lies at the distance approximately 0.2D from the compression surface

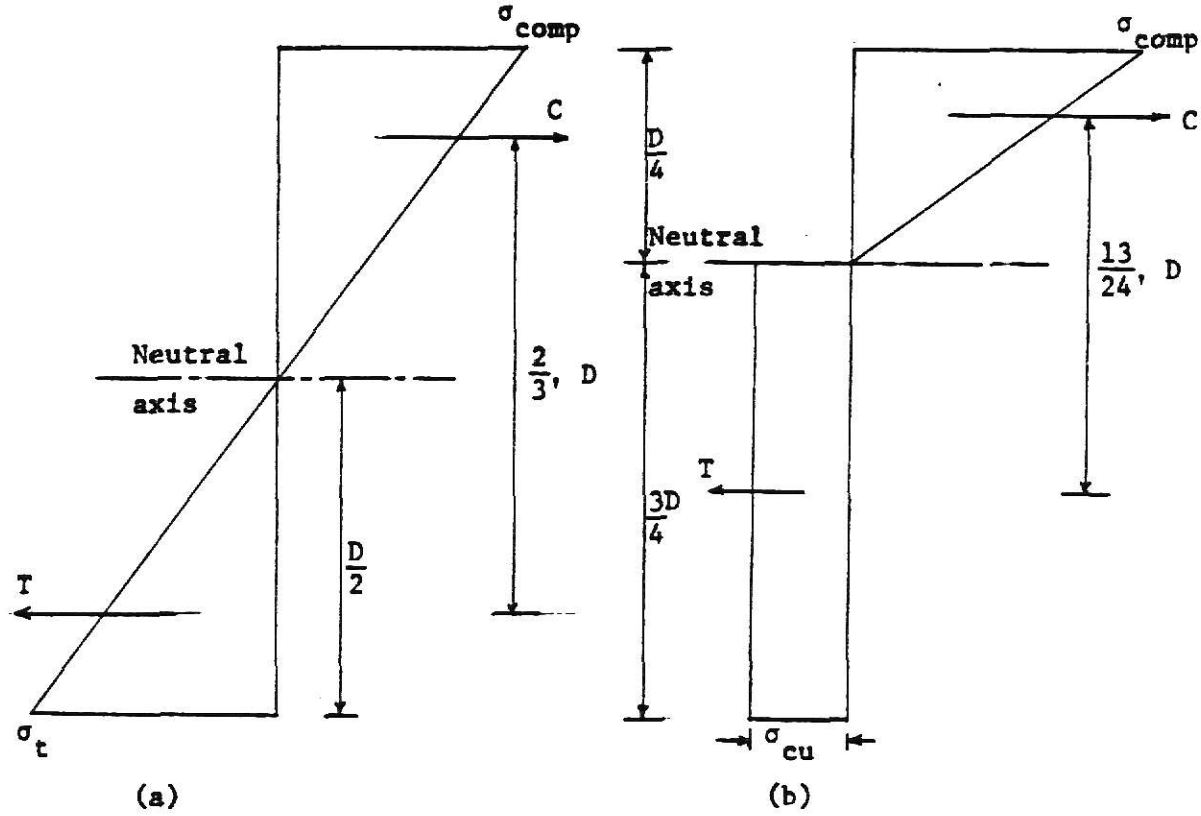

Fig. 3-3 Stress blocks in flexure (a) Elastic material. Moment of resistance = $\sigma_t \cdot D^2/6$ (b) Elastic in compression. Plastic in tension. Moment of resistance = $\sigma_{cu} \frac{13}{32} \cdot D^2$. (1)

where D is overall depth of the section. Here we assume a conservative value 0.25D for a neutral axis and assess the post-cracking flexural behavior of fiber cement composites.

In Figure 3-3 (a) equilibrium gives, forces T = C

$$T = \frac{\sigma_t}{2} \cdot \frac{D}{2} = \sigma_t \cdot \frac{D}{4} .$$

$$\text{Lever arm } L_a = \frac{2D}{3} ,$$

Hence,

$$\text{moment of resistance} = \sigma_t \cdot \frac{D}{4} \frac{2D}{3}$$

$$= \frac{\sigma_t D^2}{6} . \text{ ---------- (3-11)}$$

In Figure 3-3 (b), let σ_{cu} be the force per unit area of section carried by the fibers, which is the same as the post-cracking tensile strength in a direct tension test.

$$T = \sigma_{cu} \frac{3D}{4} ,$$

$$\text{Lever arm } L_a = \frac{1}{2} \cdot \frac{3D}{4} + \frac{2}{3} \cdot \frac{D}{4}$$

$$= \frac{13D}{24} .$$

Hence,

$$\text{moment of resistance} = \sigma_{cu} \frac{3D}{4} \cdot \frac{13D}{24}$$

$$= \sigma_{cu} \frac{13}{32} D^2 . \text{ ---------- (3-12)}$$

In order that the beam represented by Figure 3-3 (a) and Figure 3-3 (b) have the same strength, equation (3-11) must be equated to equation (3-12);

$$\frac{\sigma_t \cdot D^2}{6} = \sigma_{cu} \frac{13}{32} D^2 ,$$

Hence,

$$\sigma_{cu} = \frac{16}{39}\,\sigma_t = 0.41\,\sigma_t .$$

This enables us to state that flexural strengthening occurs when the post-cracking strength for large strains exceeds $0.41\,\sigma_t$.

Figure 3-4 (a) (1) shows that there is no decrease in flexural load capacity or moment of resistance after cracking. Figure 3-4 (b) more or less represents glass reinforced cements where the critical fiber volume for direct tension has just been met, and the calculated modulus of rupture is about 2.4 times the measured direct tensile strength. When the neutral axis reaches the compression surface of the beam, and the maximum post-cracking tensile strength of the composite σ_{cu} is achieved throughout the section depth the limiting condition occurs and

$$\sigma_{cu} \cdot D \cdot \frac{D}{2} = \frac{\sigma_{MR}\, D^2}{6},$$

$$\frac{\sigma_{MR}}{\sigma_{cu}} = 3.$$

This proves that the maximum ratio of modulus of rupture/tensile strength = 3. In practice a compression failure always starts appearing at the outer beam surface and hence this maximum ratio cannot be achieved.

3.8 Effect of Loss of Ductility in Tension on the Modulus of Rupture (MOR)

The failure strain for some fiber composites, notably GRC is time dependent and it continuously declines with age. This does not necessarily indicate that the failure strain of fibers decrease but the bond between the fiber and the matrix improves as the hydration proceeds. The bond improvement takes place due to the deposition of hydration products and thereby increase in the contact area and the interfacial frictional

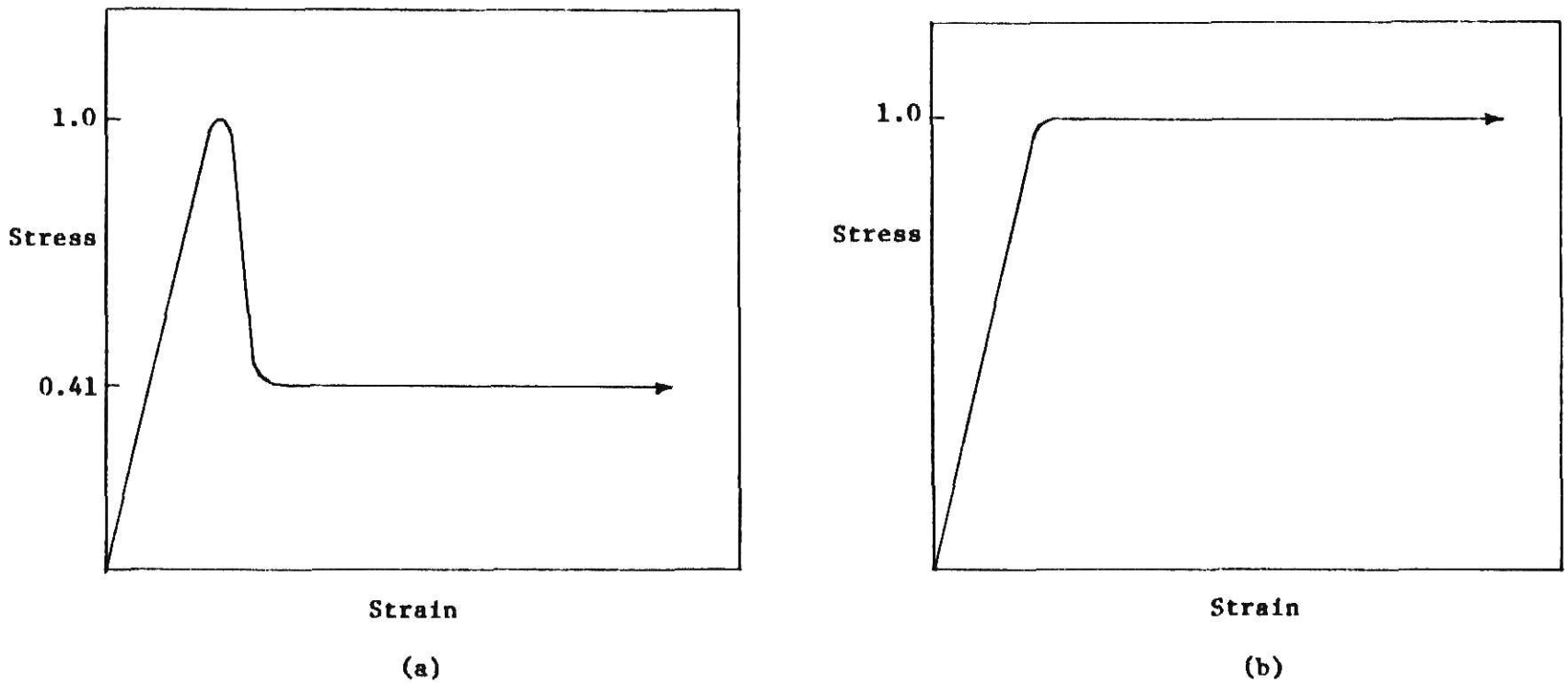

Fig. 3-4 Stress-strain curves in uniaxial tension (a) No decrease in flexural load capacity after cracking, (b) Load capacity after cracking = 2.4 times cracking load for (compressive strength)/(tensile strength) >6. (1)

forces. The composite strength is influenced by the increase in bond. The reduction in flexural strength may be caused by the reduction in composite tensile failure strain due to bond improvement between the fiber and the matrix.

In order to get the stress block similar to that shown in Figure 3-3 (b), the strain distribution in flexure must correspond to that shown in Figure 3-5 (a) (1) with a strain value of 18 ε_x in tension. The stress block shown in Figure 3-5 (a) will satisfy this condition maintaining the maximum tensile load in fiber at the outer surface of the beam at the same time. Hence, the moment of resistance of the section will be given by 0.41 σ_{cu} D^2 (Equation (3.12) and Figure 3-6 (a))(1). Refering to Figure 3-5 (b) the outer fibers start breaking at a strain of 6 ε_x and hence for the material characterized by that shown in Figure 3-5 (b) we cannot achieve a strain capacity similar to that given in Figure 3-3 (b). Hence, the content in Figure 3-6 (b) represents the corresponding stress block, and thereafter the load capacity is likely to decrease, as the outer tensile material with the largest level arm will no longer sustain load. The moment of the resistance for the stress block shown in Figure 3-6 (b) is estimated by 0.35 σ_{cu} D^2. From this it can be concluded that 15 percent reduction in load capacity can be obtained, since values of σ_{cu} are equal for both the composites.

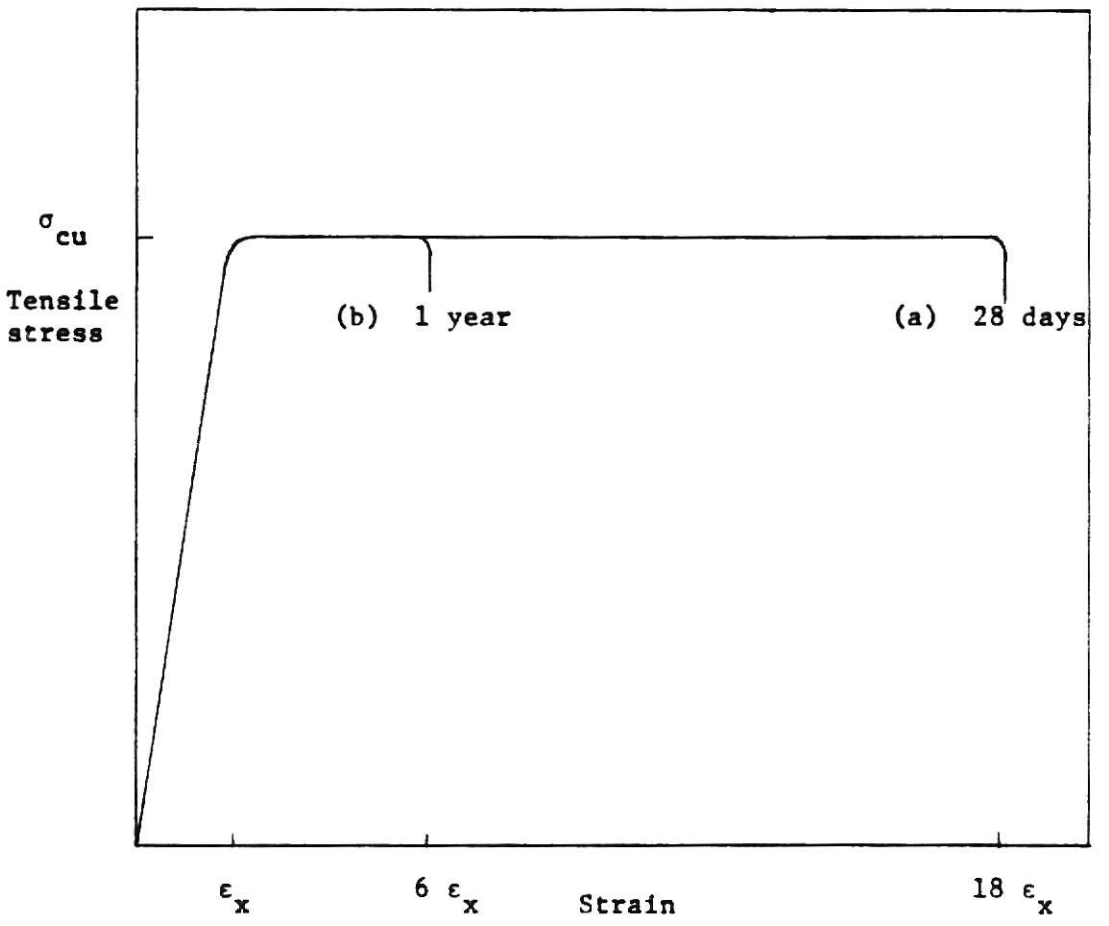

Fig. 3-5 Idealized direct tensile stress-strain curve for fiber cement. ε_x is the strain at the start of major multiple cracking at the bend over of the stress-strain curve to near horizontal. (1)

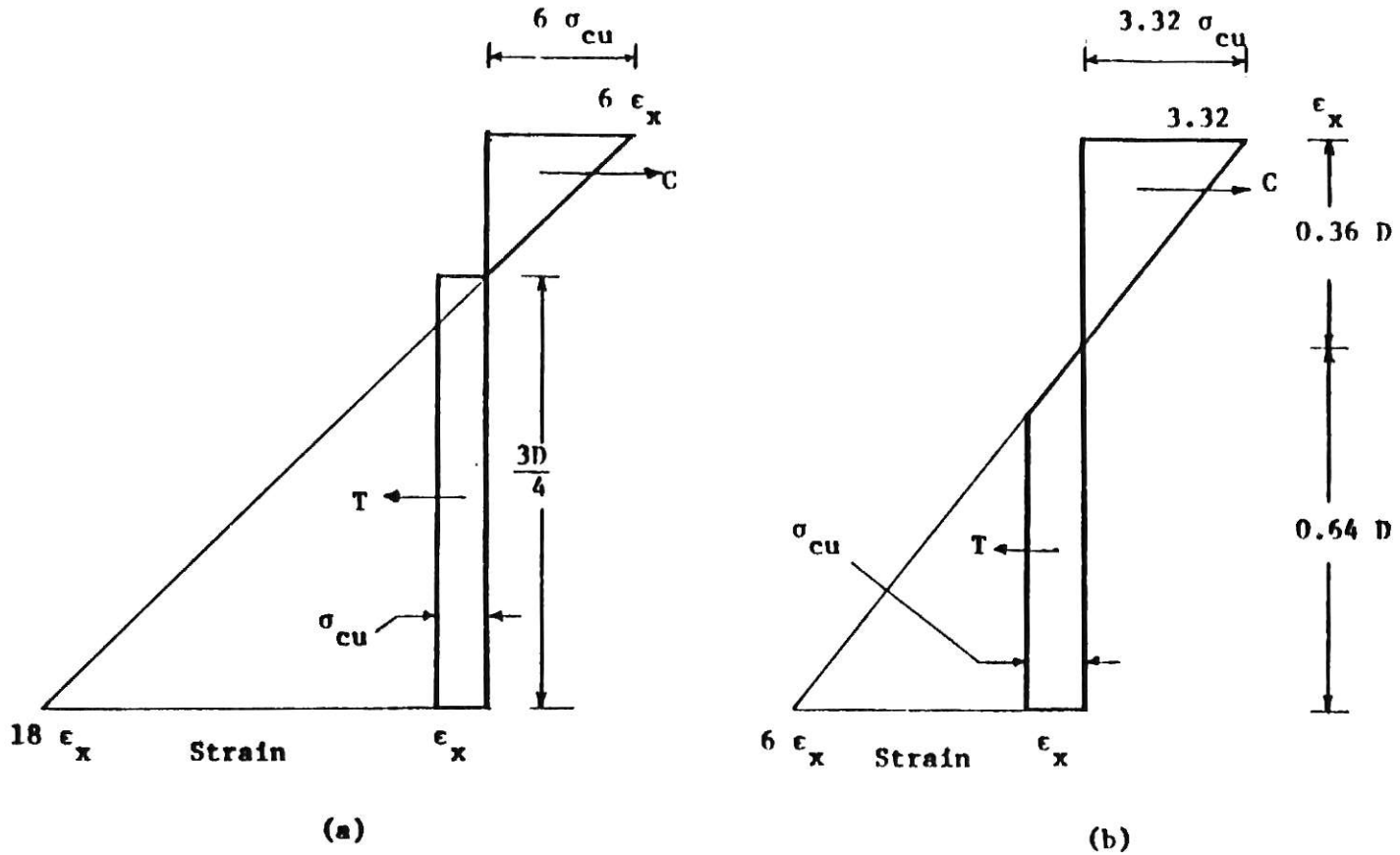

Fig. 3-6 Strain and stress distributions in flexure for the tensile stress-strain curves in Fig. 3-5 (a) For curve (a) in Fig. 3-5, moment of resistance = $0.41\ \sigma_{cu}D^2$ (b) For curve (b) in Fig. 3-5, moment of resistance = $0.35\ \sigma_{cu}D^2$. (1)

Chapter 4

ANALYSIS EXAMPLE

Statement

Calculate the modulus of rupture for the one year old glass reinforced cement, if the strain at failure is 1020×10^{-6} m/m.

$E = 20\ GN/m^2$ (assumed same for tension and compression).

$\sigma_{cu} = 10\ MN/m^2$.

Solution

We will assume the following idealized tensile stress-strain curve.

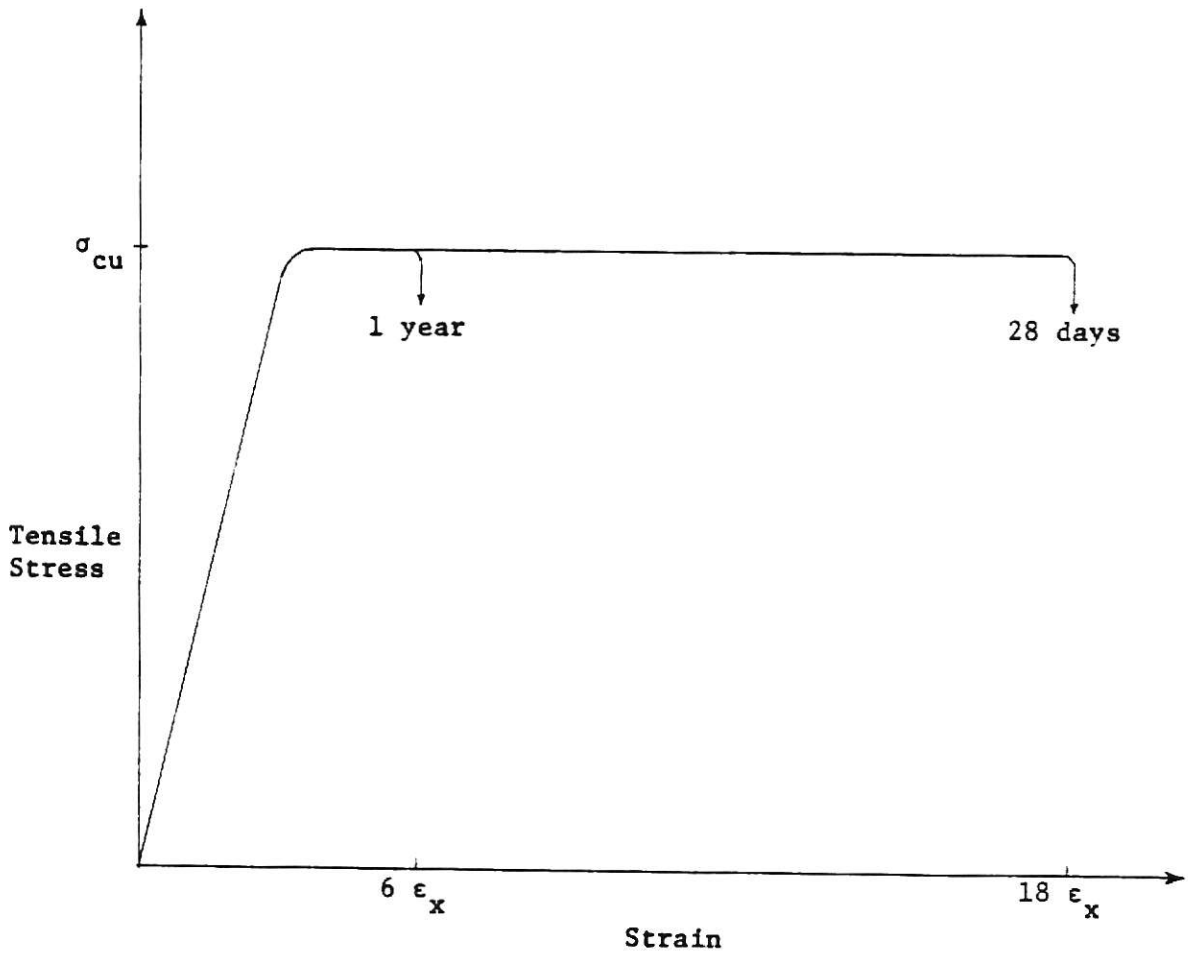

Fig. 4-1 (1) Idealized Tensile Stress-Strain Curve

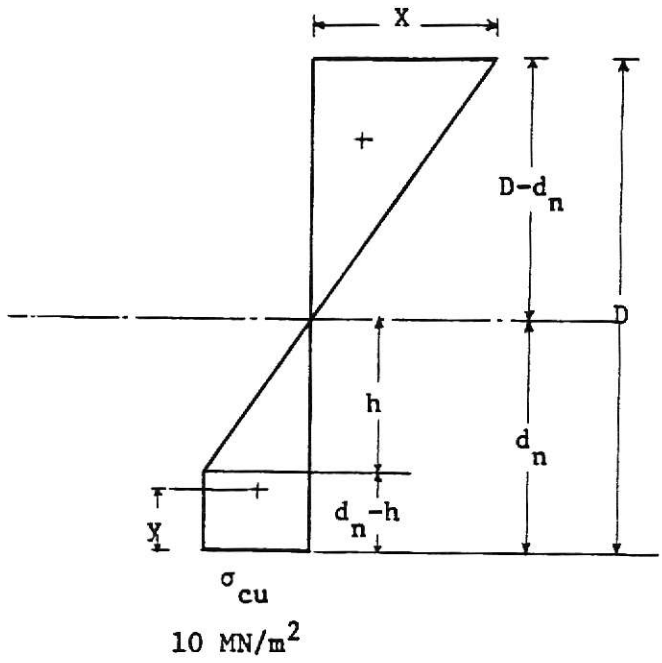

Fig. 4-2 (1) Stress Block

Here parameters X, h, d_n, y and D are defined as shown in the figure above.

Tensile failure stress = σ_{cu} = 10 x 10^6 N/m^2. Equating areas above and below the neutral axis in the stress diagram,

$$\frac{1}{2}(D-d_n)X = (\frac{1}{2} \times 10 \times h) + \{10 \times (d_n-h)\} \quad \text{---------- (4-1)}$$

The failure stress corresponding to failure strain of 1020 x 10^{-6} m/m is

$$(1020 \times 10^{-6})(20 \times 10^9 \text{ N/m}^2)$$
$$= 20400 \times 10^3 \text{ N/m}^2$$
$$= 20.4 \times 10^6 \text{ MN/m}^2$$

From similar triangles

$$\frac{10}{h} = \frac{X}{D-d_n} = \frac{20.4}{d_n} \quad \text{---------- (4-2)}$$

$$\therefore h = \frac{10}{20.4} d_n$$
$$= 0.49\, d_n.$$

Substituting h in equation (4-1)

$$\frac{1}{2} X (D-d_n) = (\frac{1}{2} \times 10 \times 0.49\ d_n) + \{10 \times (d_n - 0.49\ d_n)\},$$

$$\therefore X(D-d_n) = 4.9\ d_n + 20\ d_n - 9.8\ d_n,$$

$$\therefore X(D-d_n) = 15.1\ d_n. \text{ ---------- (4-3)}$$

From equation (4-2)

$$X = \frac{20.4\ (D-d_n)}{d_n}. \text{ ---------- (4-4)}$$

Substituting X in equation (4-3)

$$\frac{20.4\ (D-d_n)}{d_n} (D-d_n) = 15.1\ d_n,$$

$$\therefore 20.4\ (D-d_n)^2 = 15.1\ d_n^2.$$

On simplification we get,

$$5.3\ d_n^2 - 40.8\ Dd_n + 20.4\ D^2 = 0.$$

Solving d_n in terms of D, we have,

$$d_n = 0.538\ D.$$

Substituting d_n in equation (4-4),

$$X = \frac{20.4\ (D-0.538\ D)}{0.538\ D}$$

$$= 17.52\ MN/m^2$$

$$= 1.752\ \sigma_{cu}.$$

<u>To Find Lever Arm</u>

Let y be the distance of the C.G. of the tensile stress block to the farthest fiber in tension.

Taking moments about C.G.

$$(10 \times y) \cdot \frac{y}{2} = (0.274D-y) \times 10 \times \frac{(0.274D-y)}{2} + \frac{1}{2} \times 10 \times 0.264D \ (0.274D-y + \frac{0.264D}{3}).$$

$$\therefore y^2 = (0.274D-y)^2 + 0.264D \ (0.362D-y)$$

$$= 0.075D^2 - 0.548Dy + 0.096D^2 - 0.264Dy + y^2.$$

$$0.812y = 0.171D,$$

$$\therefore \ y = 0.211D.$$

Distance of CG of tensile stress block from N.A.

$$= 0.538D-y$$

$$= 0.538D - 0.211D$$

$$= 0.327D.$$

$$\therefore \text{Lever arm} = 0.327D + \frac{2}{3} (0.462D)$$

$$= 0.635D.$$

$$\therefore \text{Moment of resistance} = \frac{1.752 \ \sigma_{cu} \times 0.462D}{2} \times 0.635D$$

$$= 0.257 \ \sigma_{cu} \ D^2.$$

From equation (3.11),

$$\frac{\sigma_{MR}}{6} = 0.257 \ \sigma_{cu},$$

$$\therefore \sigma_{MR} = 6 \times 0.257 \times 10,$$

$$\sigma_{MR} = 15.42 \ MN/m^2.$$

Chapter 5

EXPERIMENTAL MECHANICAL PROPERTIES OF GLASS FIBER REINFORCED CEMENT

As the usage of the alkali-resistant glass fiber for fiber reinforced concrete is expected in the near future, experiments were conducted to get a fundamental understanding of the mechanical behavior of the GRC. Several factors affecting or contributing to the mechanical properties of GRC were studied. They are discussed one by one as below.

5.1 Effect of Glass Fiber Length and Content

5.1.1 Experimental details - Mechanical properties of a glass fiber composite are highly influenced by the glass fiber content and its dimensions. The experimental work discussed here was reported by the Building Research Establishment, UK (4). The CEM-FIL--a trade mark of Pilkington Brothers Ltd.--glass fibers of 34 mm. length were used. A batch of ordinary Portland cement was selected for all the tests. A glass roving having 30 strands, each containing 204 filaments was used for fibers. The diameter of an individual filament was 10 to 12 μm. The testboards of the size 1.5m x 1m with 10 mm. thickness were cast by employing the automated spray suction technique. The fiber lengths chosen were 10, 20, 30 and 40 mm. By adopting the spray process a random two dimensional fiber distribution in the plane of the boards was achieved. The glass fiber content was determined theoretically by the amount of glass used in fabrication and practically verified by weighing the glass fibers obtained

by washing test areas of a green demoulded board. The excess water was extracted at a suction of 70-80 KN/m^2 over five minutes. The 1.5m x 1m strips were sawn to give 150 mm. x 50 mm. test coupons. The wet curing process for 7 days followed by the subsequent curing for 21 days in water at 18°C or in air of 40 percent relative humidity at 18°C. Tensile and four point bend tests were performed on a Universal Instron testing machine. An extensometer of 50 mm. gauge length was used for strain measurement purpose. Six specimens were tested for bending, and the average value was considered.

The experimental results and relative discussion are summarized as shown. The various quantities affected by the fiber length and content are discussed separately.

5.1.2 Effect of fiber length and content on density - The principal determinants of the properties of GRC are fiber length and content, composite density, inert filler content, and fiber orientation. Also curing condition, water-cement ratio and degree of compaction indirectly influence the composite properties.

Figure 5-1 shows how the density of GRC is affected by fiber volume. According to the plot, as the fiber volume increases, for all the different lengths of fibers, density decreases, i.e., porosity of the composite increases. The glass fiber strands consisting of 204 individual filaments themselves have a built-in porosity and the contribution of this built-in porosity to the total porosity of the composite is dependent

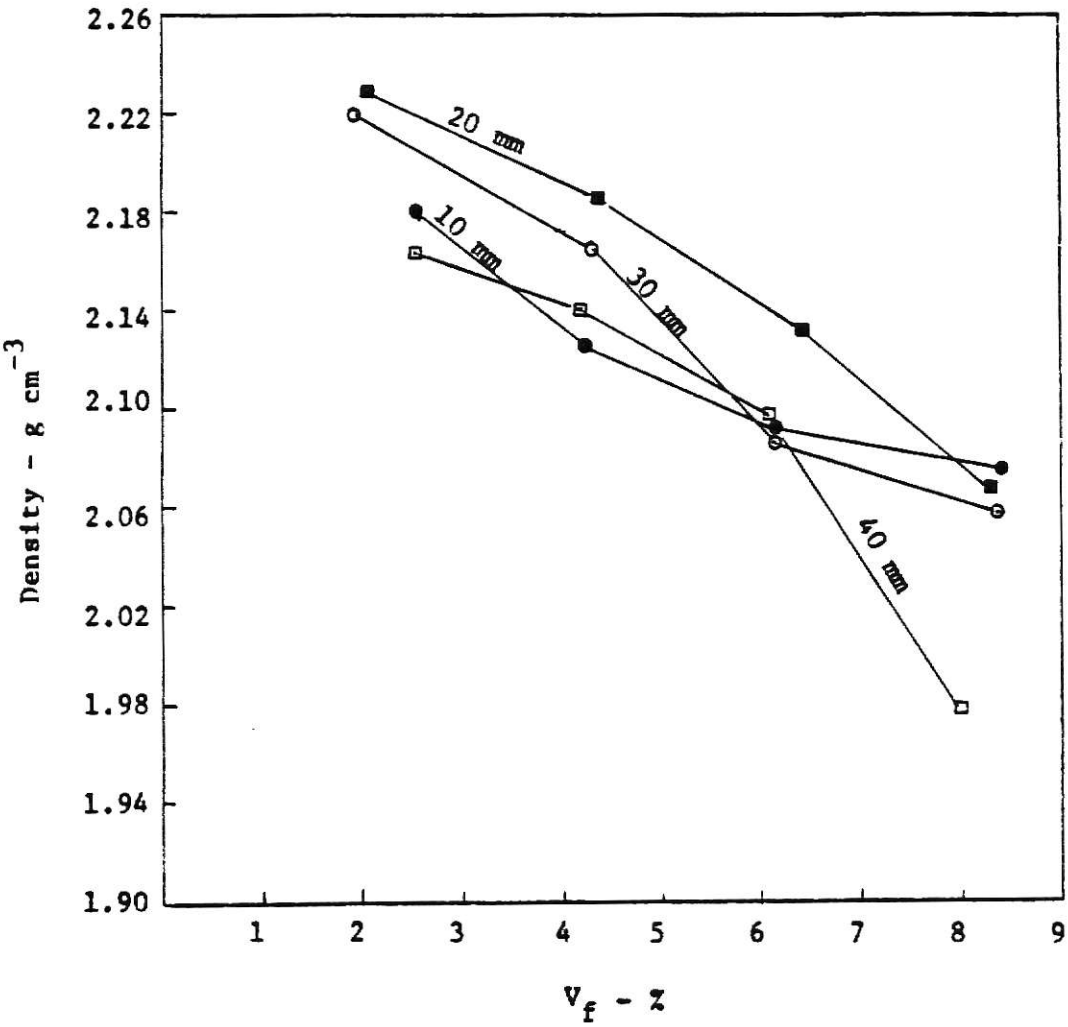

Fig. 5-1 Relation between fiber volume fraction and density of GRC composites at 28 days for different fiber lengths. (4)

on fiber length and content. Considering all the manufacturing factors. For such a composite there should be an upper limit of fiber content which prohibits the effective use of the reinforcing characteristics of fibers. For GRC manufactured by the spray-suction method, this optimum effective fiber content was suggested to be 6 percent by volume and the optimum length of fiber a little less than 40 mm.

Figure 5-2 shows a graph of Young's modulus vs. density of GRC. It is quite obvious that decrease in density causes decrease in Young's modulus. If we try to combine the conclusions of Figures 5-1 and 5-2, then an increase in fiber content should be accompanied by decrease in Young's modulus of GRC. But, practically the effect of increase in fiber content has a little effect on Young's modulus because of the low percentage of fiber.

5.1.3. Effect of fiber length and content on tensile strength - Figure 5-3 (2) shows the 28-day strength values of GRC composites containing different fiber contents. Figure 5-3 (a) and Figure 5-3 (b) represent the results for air-cured testing specimens and water-cured testing specimens, respectively. These plots indicate that the increase in fiber lengths cause the increase in tensile strengths for a given fiber content. It can further be noted that for most fibers the tensile strength capacities increase with the increase in fiber volume. But these values acquire their maxima at an approximate fiber content of 6 percent and the further increase in fiber content may decrease the tensile strengths drastically. Because after an optimum value of fiber content is reached, further increase in fiber content brings the increase in

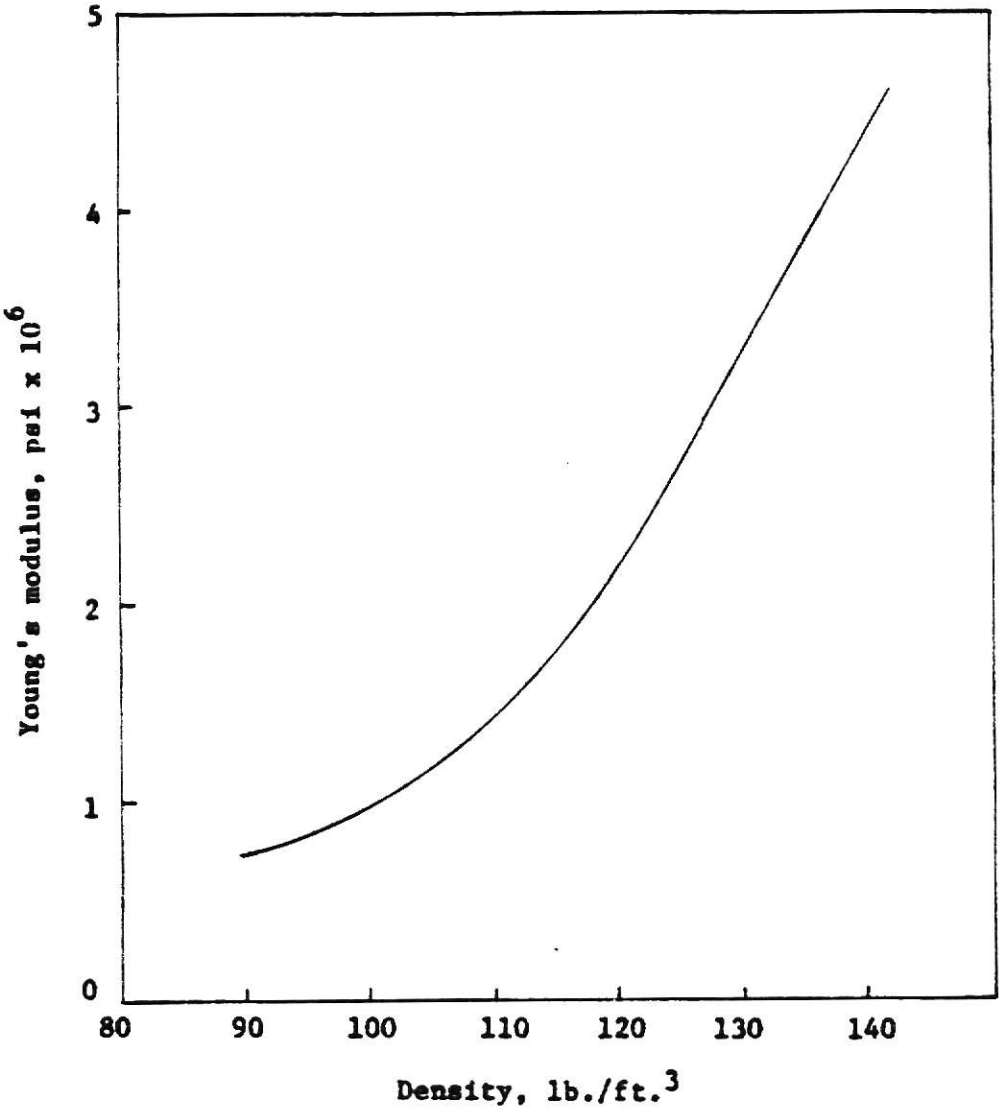

Fig. 5-2 Effect of density on Young's modulus of elasticity of GRC. (3)

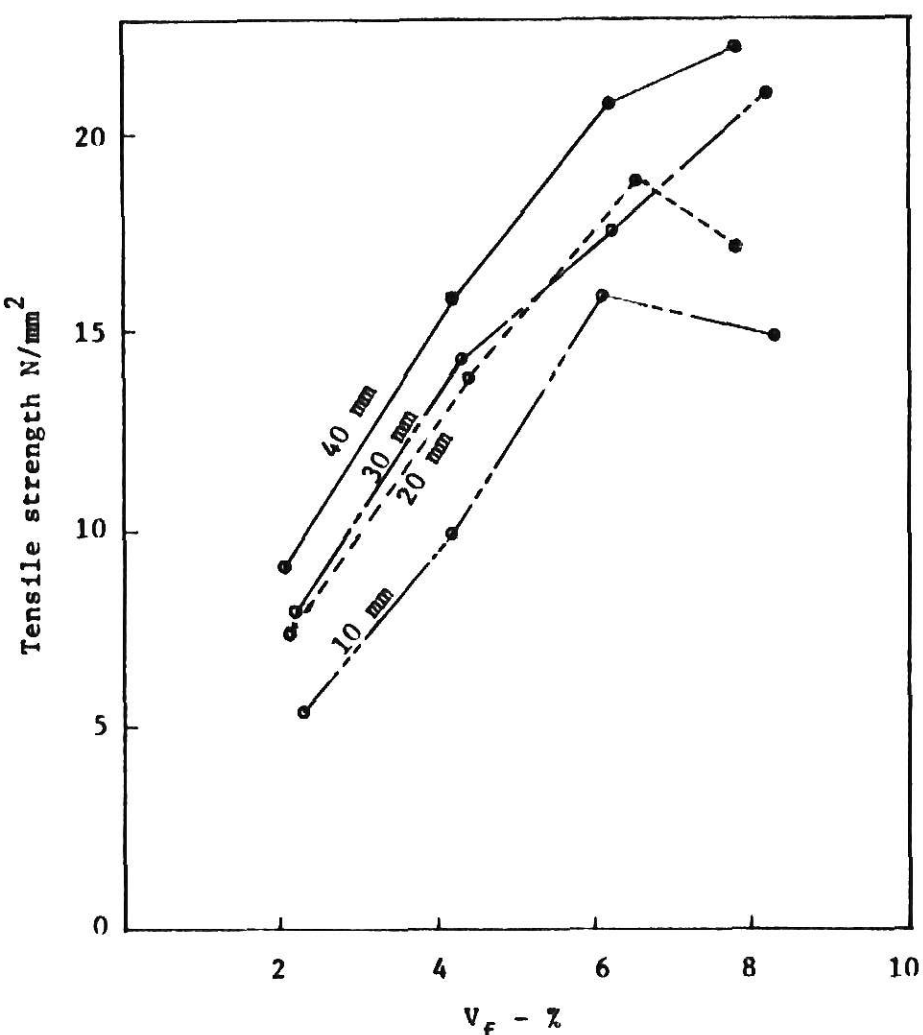

(a) Stored in air

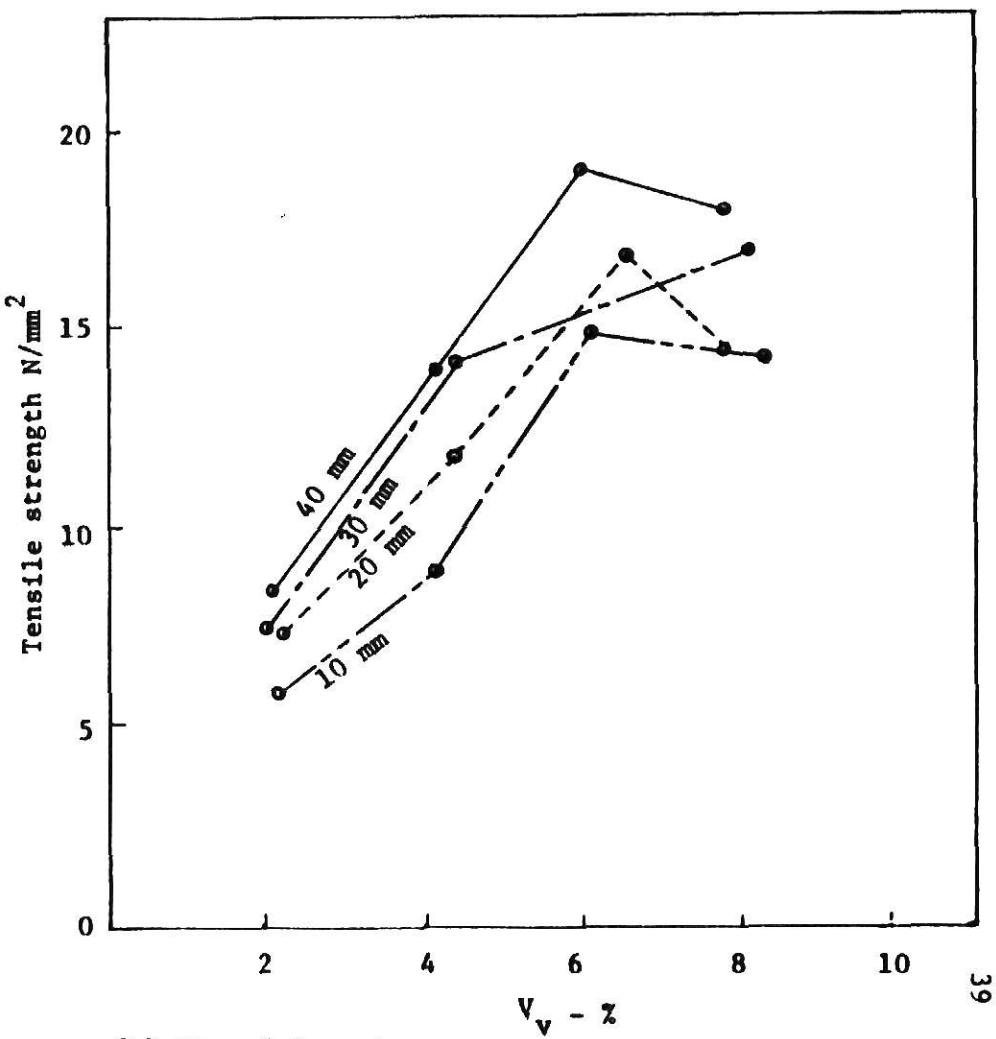

(b) Stored in water

Fig. 5-3 Relation between fiber volume fraction and tensile strength of glass fiber cement at 28 days for different fiber lengths. (2)

porosity of the composite. At 6 percent by volume addition of fibers, the corresponding tensile strength was improved 3 to 4 times as compared to the unreinforced matrix.

5.1.4 Effect of fiber length and content on modulus of rupture - For elastic materials MOR and UTS are ideally equal. That is not the case with GRC. For fiber cement composite the value of MOR is normally two to three times greater than that of UTS. The effect of fiber length and content on MOR is similar to that on tensile strengths and same conclusions can be drawn. Here also a limit of fibers beyond which fiber addition does not improve the strength of the composites is approximately around 6 percent by volume. This limit is governed by fiber characteristics as well as the fabrication method. At the optimum level of fiber addition, namely 6 percent by volume, the MOR values for GRC composites after 28 days were 4 to 5 times greater than that of the unreinforced matrix.

5.1.5 Effect of fiber length and content on impact strength and fracture energy - Figure 5-5 (1) shows the variation of the impact strength with the fiber length and content. As the fiber content increases the impact strength for all the fiber lengths increases. Here the optimum level of fiber content lies around 8 percent by volume, for both air cured and water cured specimens. This increase in the optimum level can be explained by the fact that increase in fiber content increases the porosity of the composite. But the increased porosity is advantageous here as it reduces the interfacial bond--strength. Hence, larger

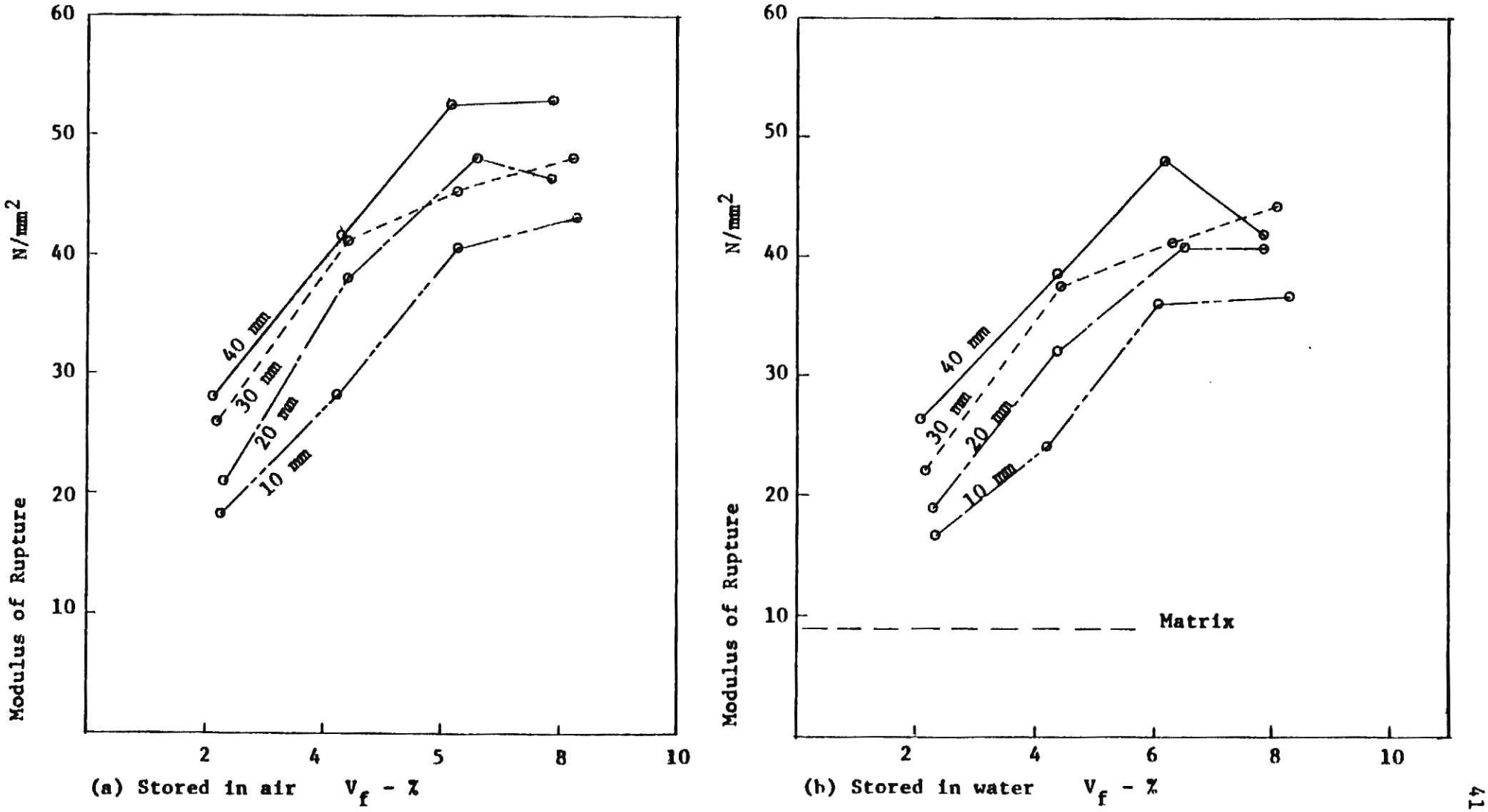

Fig. 5-4 Relation between fiber volume fraction and modulus of rupture of glass fiber cement at 28 days for different fiber lengths. (2)

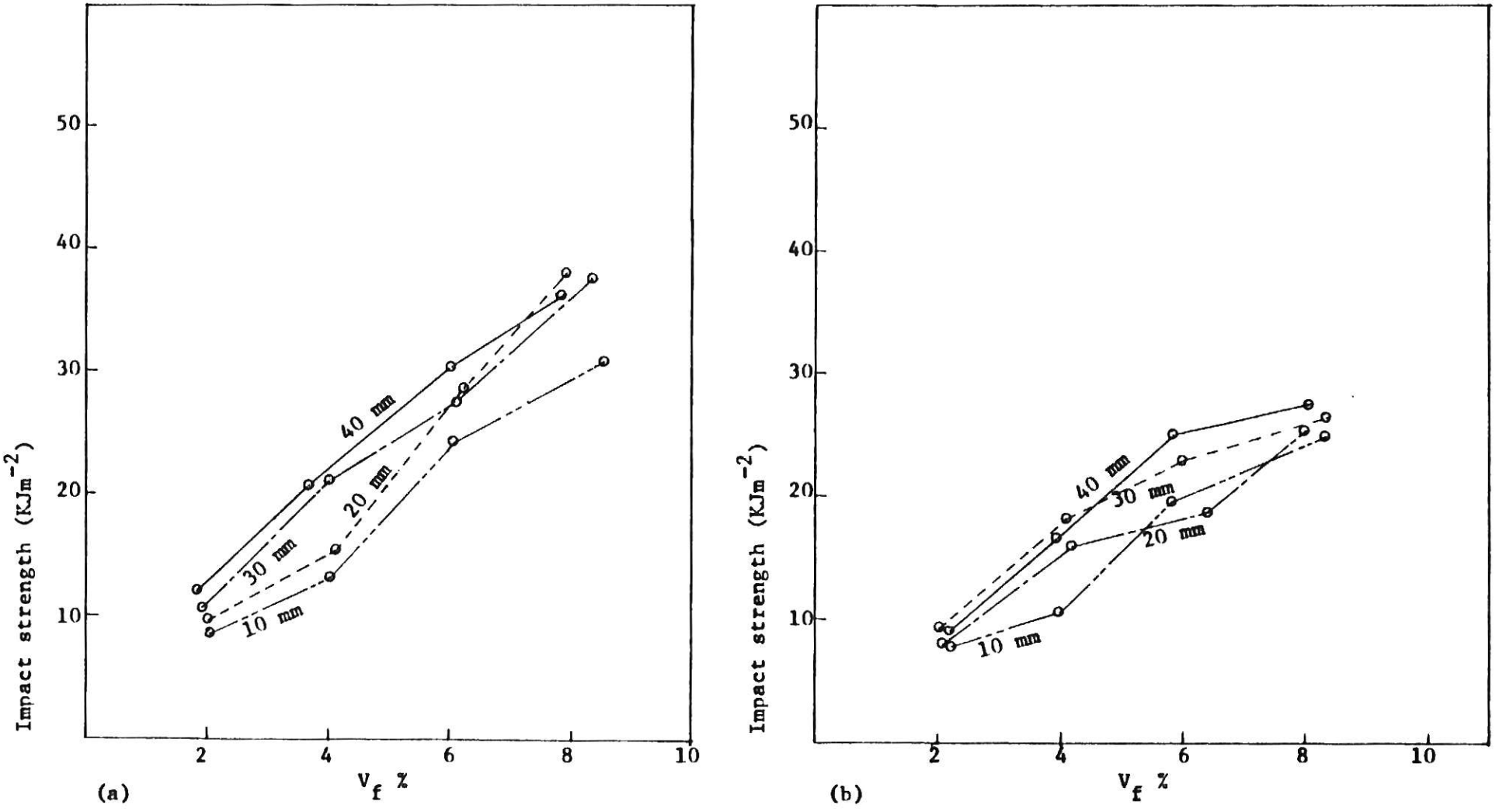

Fig. 5-5 Relation between fiber volume and impact strength of glass reinforced cement at 28 days (a) Stored in air (b) Stored in water. (1)

fraction of the fiber becomes available for pull out which is responsible for the work of fracture or the fracture energy, of brittle matrix composite. The 6 percent by volume glass fibers addition improves the 28-day impact strength of GRC by 15 to 20 times as compared to the unreinforced matrix. The impact strength seems to be increased with the increase in fiber length. The higher impact strength of the air cured specimens compared to the water cured specimens can also be explained. For water cured specimens the degree of hydration being larger, the products of hydration fill out the voids to a greater extent, thereby reducing the porosity, which subsequently reduces the impact strength as explained before. Also the water cured specimens are liable to subject to severe corrosion action of cement on glass fibers.

5.1.6 Effect of fiber length and content on tensile stress-strain curve of GRC - Before starting the discussion about the variation of tensile stress-strain curves with different fiber lengths and contents, let us have a glance at the ideal stress-strain behavior of GRC.

As shown in Figure 5-6 (3), the entire stress-strain curve may be divided into four regions. Part OA represents the elastic behavior range within which stress and strain are linearly related. The Point A is called the LOP. Region AB shows a bend-over range or a transition zone within which micro-cracking starts. Region BC describes the zone within which multiple cracking takes place. At Point C the cracking process has been completed. Region CD corresponds to the

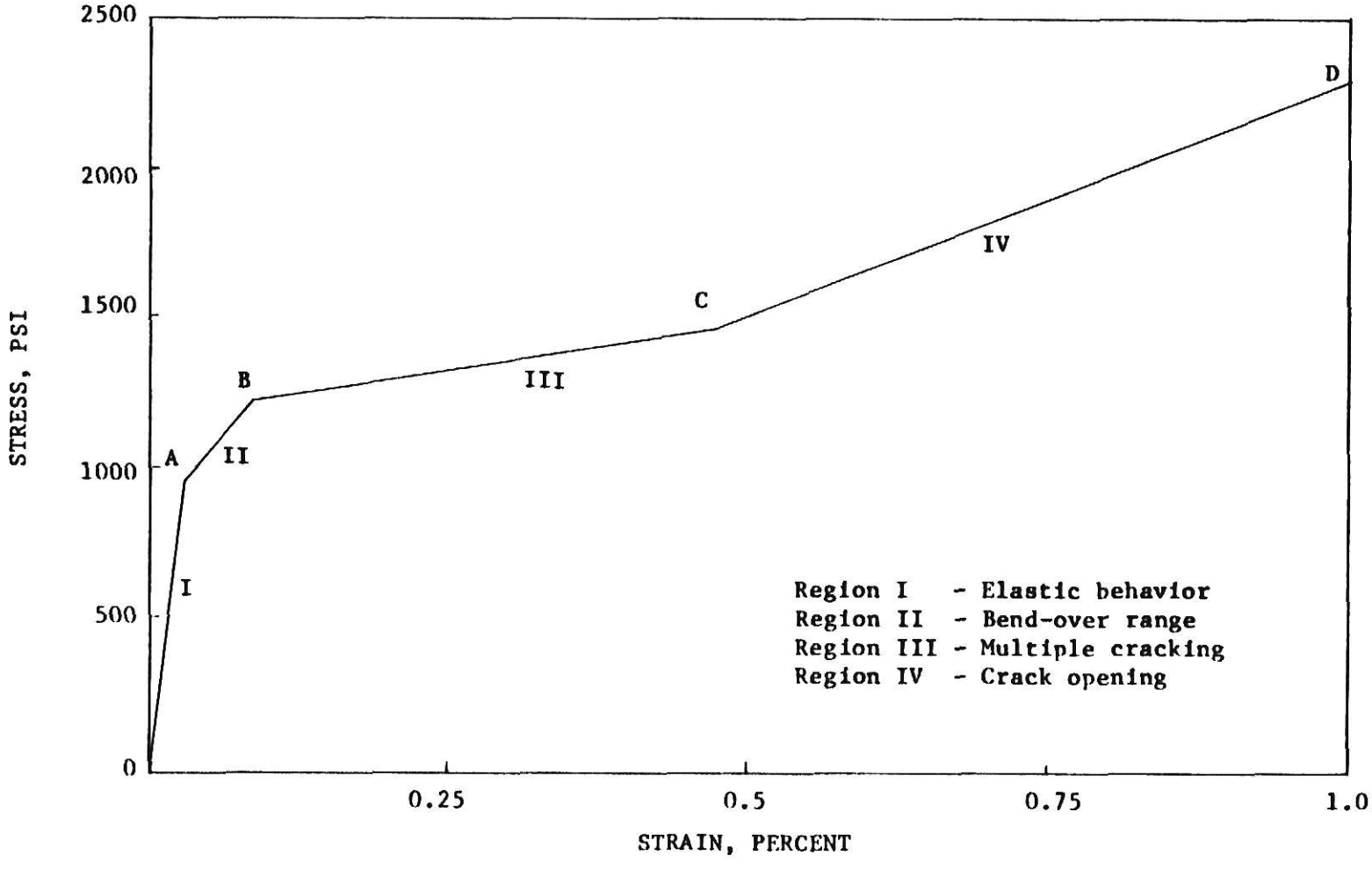

Fig. 5-6 Stress-strain behavior of GRC in direct tension. (3)

crack opening with the fibers bridging the cracks. At this stage the stress in the composite is taken by the fibers either by the elastic extension or the pull out. Finally, at Point D called UTS, a specimen breaks completely.

Figure 5-7 (3) gives an idea about the general stress-strain behavior of GRC when subjected to compression, bending and tension. The stress-strain behavior in compression is linear even up to 8000 psi stress as shown. In bending, the material passes through all the regions as described earlier in case of direct tension. But in bending the deviation from the elastic range is observed at a comparatively higher stress. In other words, LOP is comparatively larger in bending. Also the ultimate failure point called MOR in case of bending is much higher than that of UTS--an ultimate failure point in direct tension. As mentioned earlier, this ratio of MOR/UTS ranges from 2 to 3.

Figure 5-8 (4) represents the stress-strain behavior in accordance with the fiber content for 30 mm. long fibers. It can clearly be observed that higher values of LOP are achieved as we increase fiber content. For the lower fiber contents the stress at which the multiple cracking of the matrix takes place is almost constant, but for the higher fiber contents this stress increases. This can be explained by the progressive transfer of stress across the interface. Again the stresses and the strains at LOP are comparatively higher in case of water cured specimen than that of air cured specimen, the reason being the same as mentioned earlier, that the

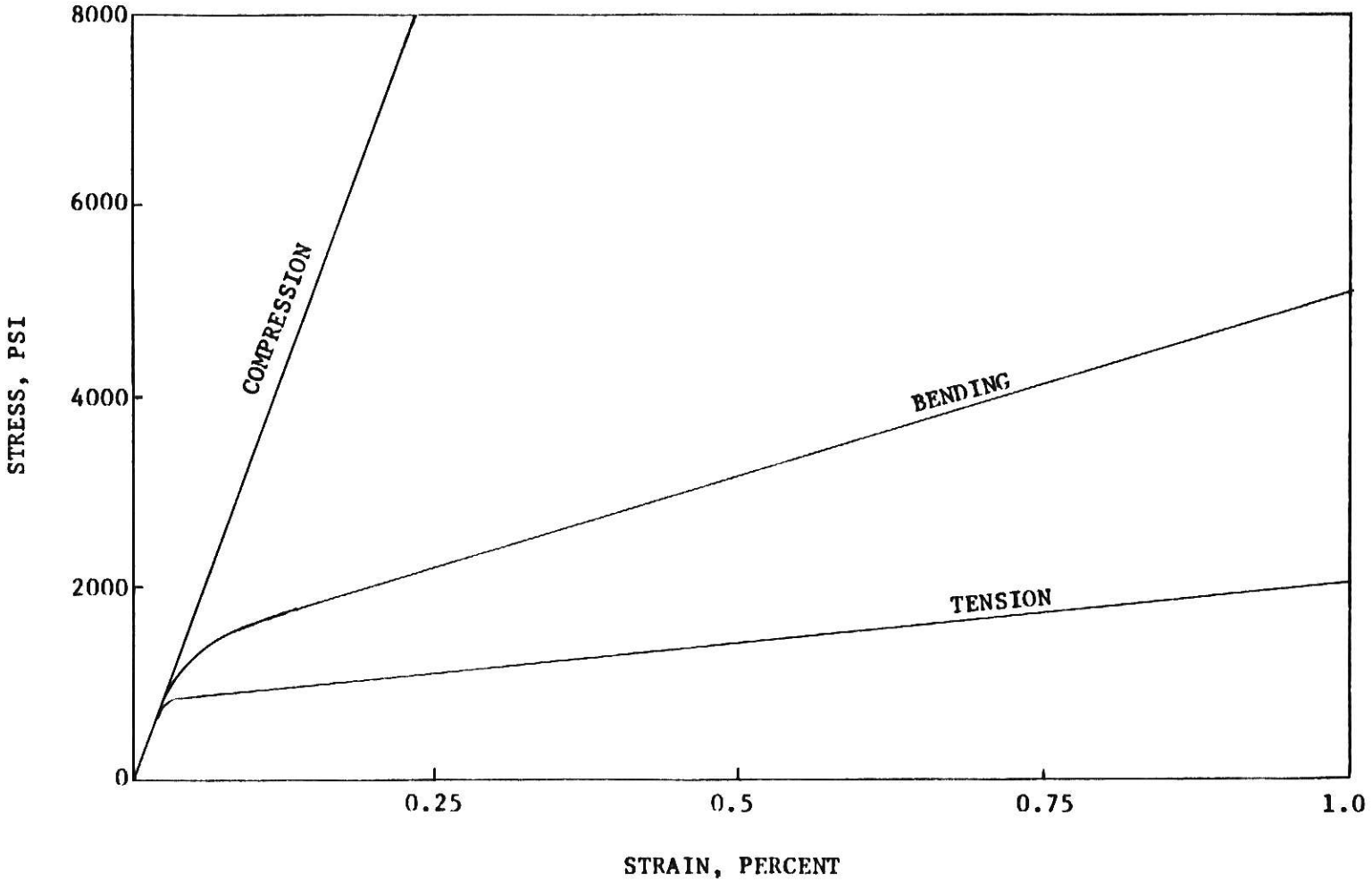

Fig. 5-7 General stress-strain behavior of GRC subject to compression, bending and tension. (3)

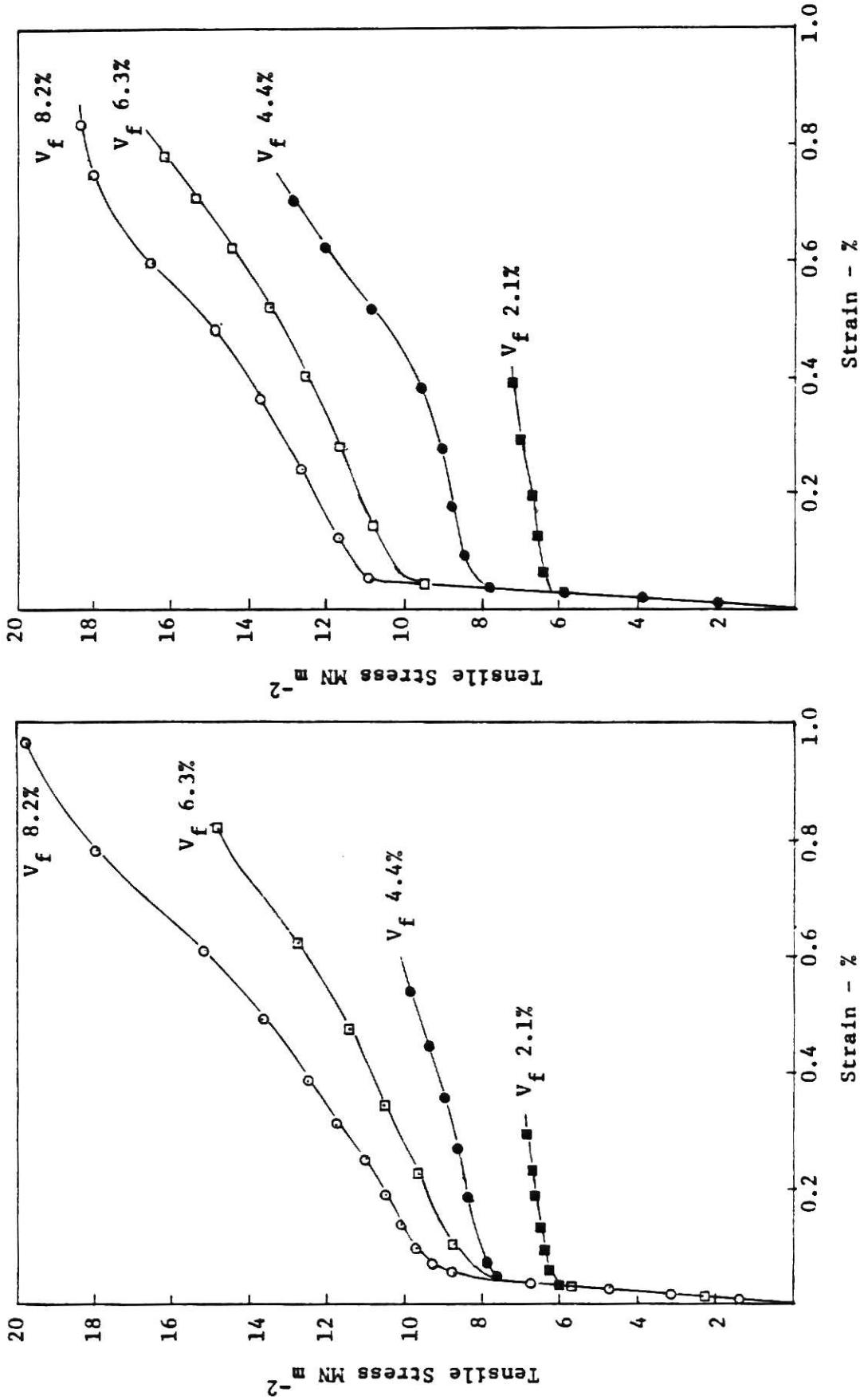

Fig. 5-8 Tensile stress-strain curves of GRC composites containing 30 mm long fibers with different fiber volume fractions at 28 days (a) Stored in air, (b) Stored in water. (4)

comparatively higher degree of hydration renders more strength to the composite in case of water cured specimen.

As shown in Figure 5-9 (4), the tensile stress-strain behavior is similar when we vary the fiber lengths keeping the fiber content constant at 4 percent by volume. The increase in fiber length increases the values of stress and strain at LOP. The greatest benefit of considerable increase in the ultimate failure stress and strain is achieved by the increase in fiber length.

5.2 Effect of Method of Manufacture

Table 5-1 (10)

Properties of composites made by four processes

(Age at test: 28 days; 20 mm. glass fibre: matrix neat Portland cement)

Method of manufacture	Spray-suction	Hand-molded premix	Extruded premix	Pressed premix
Modulus of rupture MN/m^2	21.2	9.8	18.0*	13.5
Impact strength (Charpy) KJ/m^2	8.1	8.6	9.0	9.2
Density (oven dry) $Kg/m^3 \times 10^{-3}$	2.18	1.60	1.74	1.80
Glass fibre (wt. % of dry materials	3.25	2.5	2.5	2.5
Water/cement ratio	0.30	0.40	0.26	0.10

*Tested normal to the extrusion direction.

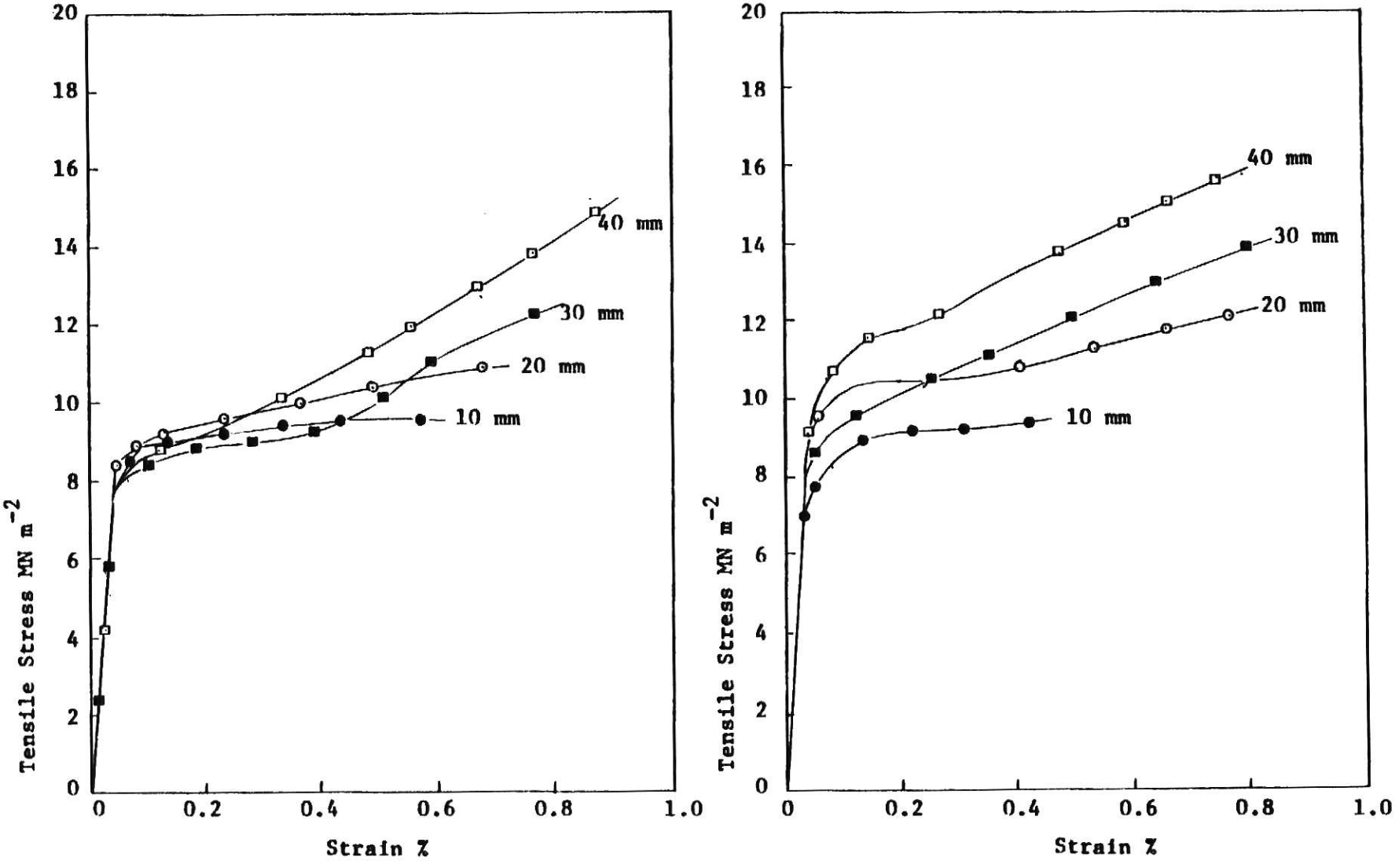

Fig. 5-9 Tensile stress-strain curves of GRC composites containing 4% fibers with different lengths at 28 days (a) Stored in air, (b) Stored in water. (4)

The method of manufacture greatly influences some of the characteristics of the GRC composites. Table 5-1 (10) exhibits various properties like MOR, impact strength and density of GRC composites manufactured by four different methods with the mentioned glass fiber content and water/cement ratio. All the test boards were stored in laboratory air for two days. During this time they were sawn to the testing size. Curing was performed at 18°C under 60 percent R.H. Testing was done after 28 days. The hand-moulded and pressed mixes contained 0.2 percent methylcellulose and the extruded mix contained 0.8 percent.

The selection of a particular method in deciding optimum properties becomes so important because that indirectly allows us to select a specific type of fiber distribution. As an example, the spray-suction technique renders us a two dimensional random in-plane fiber orientation of the composite.

In the case of the extruded product, the partial alignment of the fibers is achieved in the direction of extrusion. Hence, better results for bending strength were obtained with the spray-suction and extrusion techniques. Thus, the spray-suction process and extrusion method, both gave comparatively greater reinforcement efficiency. Impact strength did not exhibit considerable correlation with the fabricating method, but was improved for the lower density mixes and higher glass content.

5.3 Age Effect on Glass Fiber Reinforced Composite (GRC)

Since civil engineering materials are expected to last for fifty or more years, their durability study is essential. Durability means here, the degree of retention of the initial mechanical properties of a

Table 5-2 (3)

Strength properties of spray-dewatered GRC at various ages using 5 percent glass fiber (BRE data)

Properties	Total Range for Air and Water Storage Conditions at 28 Days	1 Year			5 Years			20 Years (estimated)	
		Air*	Water**	Weathering	Air*	Water**	Weathering	Air*	Water**
Bending MOR (psi)	5075-7250	5075-5800	3200-3600	4350-5200	4350-5075	3050-3600	3050-3350	3775-4900	2900-3000
LOP (psi)	2000-2550	1300-1900	2300-2800	2000-2500	1450-1750	2300-2800	2175-2610	1200-1450	2300-2610
Tensile UTS (psi)	2000-2550	2000-2300	1300-1750	1600-2000	1900-2175	1300-1750	1000-1200	1750-2175	1200-1600
BOP (psi)	1300-1450	1000-1200	1300-1600	1300-1450	1000-1200	1000-1300	1000-1200	1000-1200	1200-1600
Young's Modulus (psi x 10^6)	2.9-3.6	2.9-3.6	4.0-5.0	2.9-3.6	2.9-3.6	4.0-5.0	3.6-4.6	2.9-3.6	4.0-5.0
Impact Strength (Izod) (in.-lb/in.^{2})	85-155	90-125	40-50	65-80	90-105	20-30	20-35	70-100	20-35

*At 40 percent relative humidity and 68°F.

**At 64 to 68°F.

1 psi = 0.0069 N/mm^2

Notation: MOR -- Modulus of rupture.
LOP -- Limit of proportionality.
UTS -- Ultimate tensile strength.
BOP -- Bend-over point.

composite over a working range of age. Some of the glass fibers, namely E-glass fibers, are notoriously attacked by the alkalinity generated in the cement paste. Even the alkali-resistant fibers undergo noticeable changes under the influence of alkaline environment. This change in behavior demands a careful durability study of the GRC composites. Table 5-2 (3) shows the various strength properties of spray dewatered GRC at different ages using 5 percent glass fiber (BRE data).

5.3.1 Fiber tensile strength (15) - Figure 5-10 (2) shows a plot of fiber tensile strength vs. age in years. Cohen and Diamond (15) carried out the experiment using air stored boards at 22°C and 50 percent R.H. GRC being a newborn technology the test data is available for a limited time range. Still, attempts have been made to predict the further behavior by extrapolation of the available data. The fibers were extracted from the composite cured under different conditions and were tested for a direct tensile strength. The results proved that the corrosive effect on the fibers was comparatively severe for the wet cured specimens, whereas the dry air cured specimens exhibited little change in tensile strength.

5.3.2 Modulus of rupture - Boards of the size 4m x 1m x 10 mm were fabricated and test specimens 150 mm x 25 mm x 10 mm were sawn from boards. They were stored either in air at 18°C and 40 percent R.H. or continuously under water at 18°C. The fiber content was 5 percent with the length of fibers 34 mm.

Figure 5-11 (10) shows a plot of modulus of rupture against log time for the GRC prepared with alkali-resistant glass in

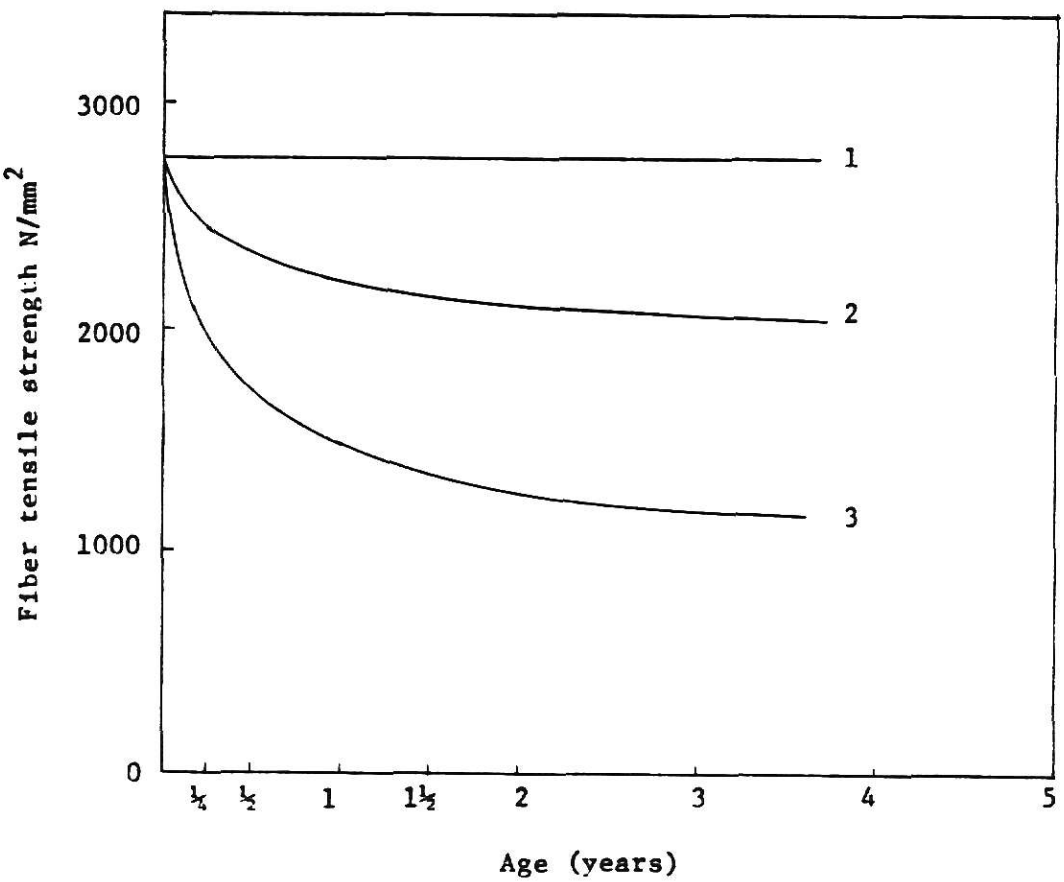

Fig. 5-10 Strength results plotted against time. (2)

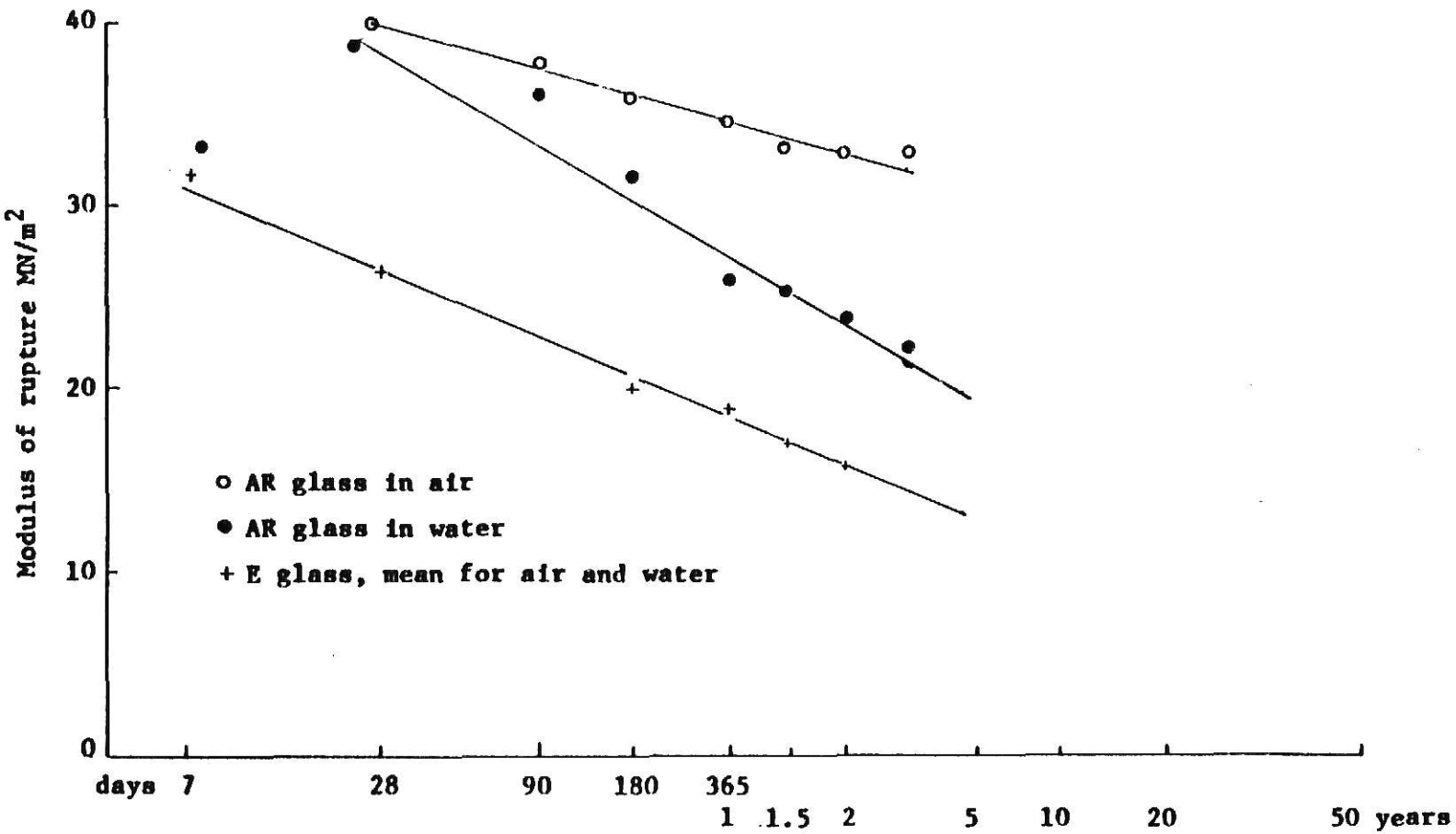

Fig. 5-11 Modulus of rupture versus log time for composites made with E glass or alkali-resistant glass. Air and water storage. (10)

water and in air (10). The results for E-glass have been combined together because of the similarity in results for the two storage conditions. An improvement in the bond between matrix and fiber causes the initial increase in strength of the composite. After 28 days the strength of the specimens gradually starts to fall down. The degree of this decreasing tendency in strength after 28 days is observed to be higher in the case of water cured specimens than that of air cured specimens. Again, a composite made out of E-glass fibers is more susceptible to this decaying action to strength as compared to the alkali-resistant glass fiber composite. The long term decrease in strength is due to decrease in glass fiber strength, but it is still controversial whether that decrease in strength is brought by residual alkali attack or mechanical damage to the fiber by crystal growth as the hydration proceeds in the cement matrix.

5.3.3 Impact strength - In order to visualize the effect of age on the impact strength of GRC let us consider Figure 5-12 (10). As in the case of MOR here also we notice an increase in strength of the composite in the beginning brought by improved bond action, but later a reduction in impact strength is observed. It can also be seen that the rate of reduction of impact strength is comparatively higher than that of bending strength. This happens because the cumulative effect of fiber weakening and changes in interfacial bond characteristics causes the fracture of fiber rather than pull out.

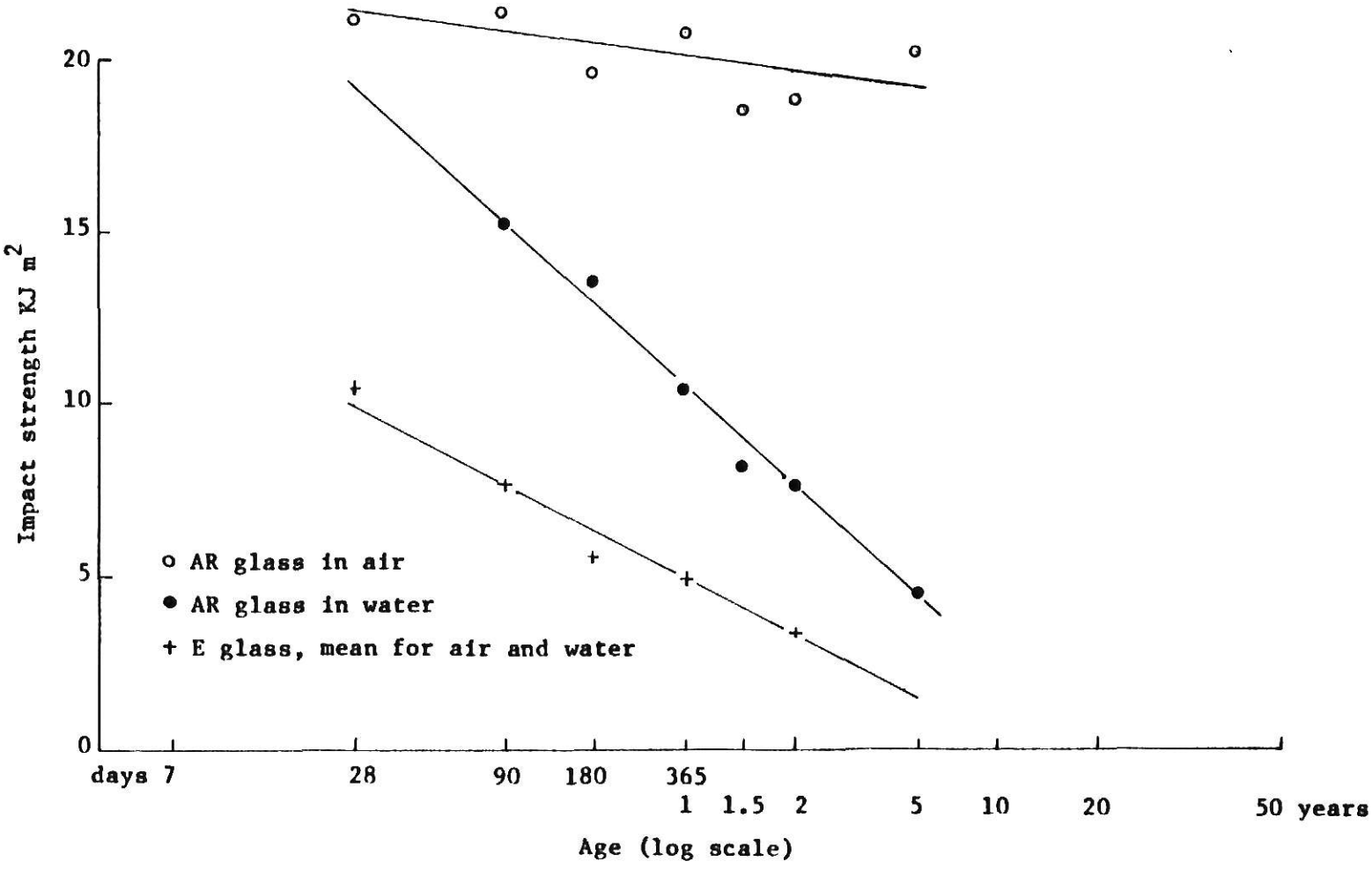

Fig. 5-12 Impact-strength versus log time for composites made with E glass or alkali-resistant glass. Air and water storage. (10)

A remedy has been suggested to this problem. The modification of the matrix and coating the glass fiber strands with a suitable material reduces the undesirable changes in fiber characteristics. The fracture toughness of GRC can also be improved by adding water-durable polymer emulsions to the cement matrix (10). Still, research is in progress to tackle this problem. It can be concluded from a reasonable extrapolation of the available data, that glass products used indoors show a little variation in material properties over a period of twenty years.

5.4 Fracture Toughness

Fracture toughness tests were carried out on the composites prepared from 2:1 OPC/Pfa mixes with 0, 2.5 and 5 percent glass fiber by weight of the dry solids. The specimens were tested at ages of 14, 28 and 84 days in the form of 250 x 38 x 38 mm. beams under four point loading. A notch with 10 mm. depth was sawn at the centre on the tensile face. The load was increased in stages and the corresponding deflection was measured. Figure 5-13 (10) shows a GRC beam with 2.5 percent glass fiber content. The crack depth was estimated from the compliance of the beam as given by the next loading cycle.

From that the critical stress intensity factor K_{1c} was calculated. As the crack growth and fiber content increased, K_{1c} also increased linearly. The effect of age at the time of testing was not observed to be affected substantially. The apparent value of K_{1c} is given by $K_a = 0.4 + 0.025\ cf$ where K_a is the apparent toughness in $MN/m^{3/2}$, c is the crack growth in mm. and f is the fiber content, percent of dry solids by weight. For $c = 0$, we get $K_a = 0.4$, that corresponds the unreinforced

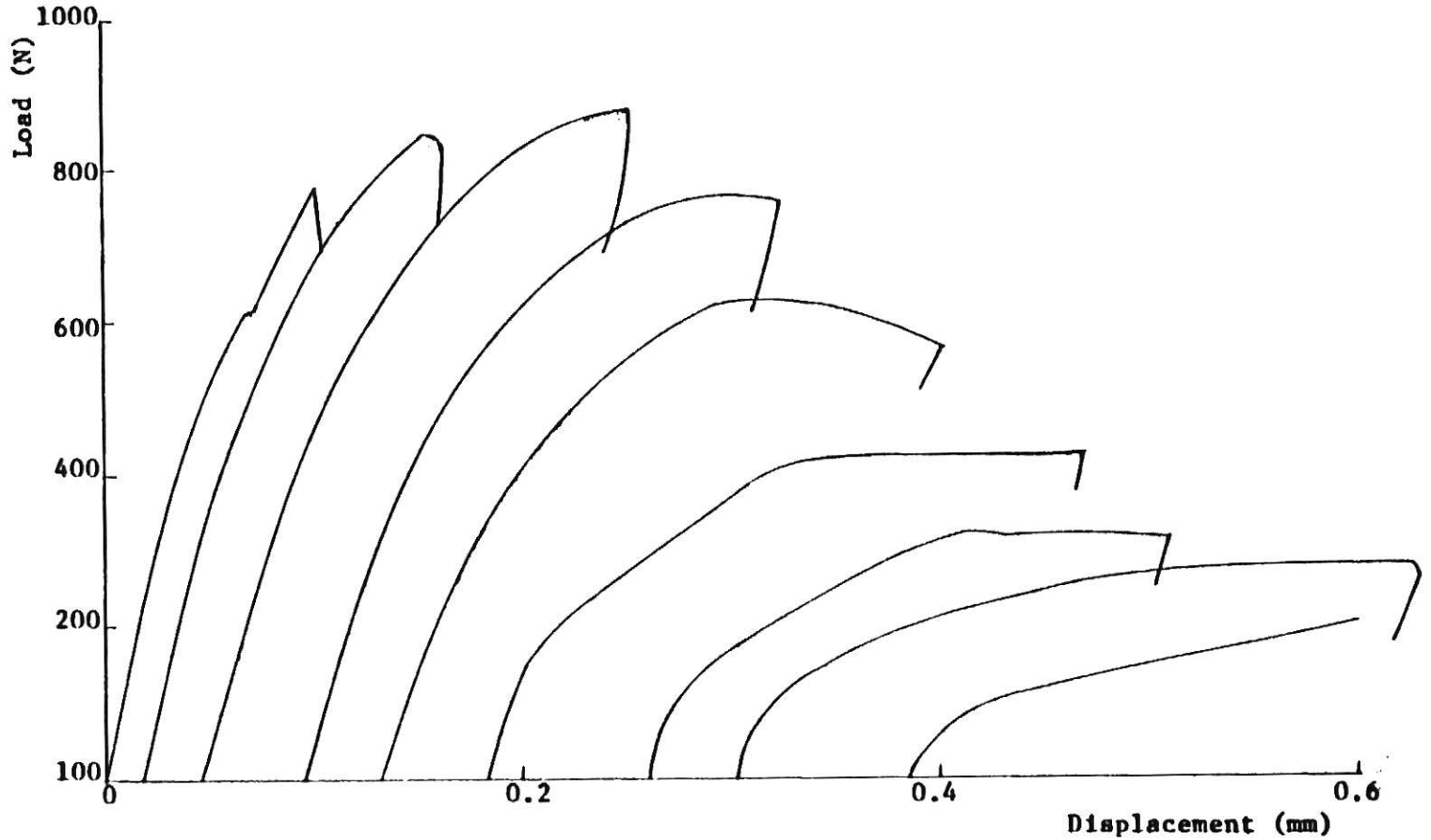

Fig. 5-13 Typical load/beam displacement result. Matrix with 2.5% glass fiber. (10)

matrix. Hence, during the development stage of cracking the toughness of the fiber reinforced composite is the same as that of the unreinforced matrix, but furthermore, with the increase in crack-growth, the toughness of the composite also increases. This leads to the crack growth arrest mechanism which is helpful in reducing failure.

5.5 Shear Strength

As mentioned earlier, the GRC composites fabricated by the spray-suction technique, have the fibers randomly distributed in the plane of the composite, and hence the shear values are dependent of the direction of load.

(1) Inter-laminar shear - Fibers do not contribute to this shear value. The inter-luminar shear value is about 300 psi. (2.07 N/mm^2)

(2) In-plane shear - Here the matrix and the components of the fibers at right angles to the line of load play a part in resisting the in-plane shear. This value is comparatively higher, namely 1200 psi. (8.27 N/mm^2)

(3) Punch through shear - The punch through shear value is fiber controlled because in resisting this shear fibers are fully utilized. The experimentally obtained value is the highest among all others, namely 5100 psi. (35.14 N/mm^2)

5.6 Shrinkage

GRC composites prepared from a neat cement paste exhibit very high shrinkage. The approximate value of ultimate initial drying shrinkage is suggested to be 0.3 percent at 122°F and 30 percent relative humidity. This shrinkage can be controlled by incorporating an inert filler like silica sand or fuel ash. Still the shrinkage is significantly larger as

compared to the precast concrete because of much higher cement content of GRC. Even though shrinkage cracking is not a common problem here, it can occur at the location of low fiber content or fiber orientation.

5.7 Creep and Fatigue

Creep properties of GRC are identical to those of concrete. The stiffening bridge action of the fiber resists the relatively high creep of the cement phase. The interaction between the matrix and the fiber are not found to be contributing to any disasterous creep effects in case of the composites.

Fatigue tests confirmed the suitability of the GRC composites subjected to cycling. For flexure, cycling between zero and a maximum stress less than the elastic limit provides a satisfactory value of 10^6 cycles for a fatigue life. The fatigue properties resemble those of asbestos cement.

5.8 Fire Resistance

GRC composites have excellent fire resistance. The bridging action of the fibers prevents the matrix from falling apart even under the most adverse situations like the complete dehydration of the matrix and thus prohibits flame penetration. Generally, water evaporation is not possible for a well compacted neat cement matrix because of its density. This may sometimes lead to explosive disintegration of the matrix, but this may be eradicated by the modification of the matrix which may subsequently reduce the density and the water content required.

Chapter 6

APPLICATIONS AND ECONOMICS

Glass fiber reinforced cement being a new construction material, its structural application is questionable. Pilkington Brothers and BRE--the pioneers of this technology suggest that unless and until the long-term working knowledge in this field is obtained, CEM-FIL fiber and GRC components should be restricted to the non-structural or the semi-structural field of application. This area of prohibition includes direct load-bearing frameworks, beams and columns, suspended floor slabs, major load bearing walls, self-supporting roofs and major water retaining structures. Research efforts are in progress to explore the possibility of using GRC in the above mentioned 'structural' areas.

6.1 Advantages

Numerous advantages associated with the applications of GRC helped it to enter the commercial market. They are listed below.

(i) With the use of spray-suction technique almost any desired shape and size can be cast. As large as 24 x 10 ft. panels have been manufactured for the Credit Lyonnais Building.

(ii) Handling and erection do not require very careful attention because of its high impact strength.

(iii) GRC products have commendable fire resistance. Even the panels with 2 hour fire resistance can be designed.

(iv) When compared with concrete, these panels are relatively light weight.

(v) A wide range of surface finishes can be obtained.

6.2 Application Areas

The various application areas are depicted in brief as below.

6.2.1 Cladding panels - Two kinds of GRC panels can be fabricated; namely, a single skin panel or a sandwich construction. Typically, the single skin panels have thickness of about 9.5 mm . Sandwich panels are formed from two skins of about 6.3 to 9.5 mm. thick, which is separated by a desired kind of core. The thickness of core mainly governs the fire rating. The first major commercial application of GRC cladding was in an eleven story block of Greater London Council Flats. GRC sandwich panels are also used for exterior facade of system built housing in South Africa. Then the use spread out to form the various odd shaped cladding panels. Even now the cladding panels are the predominant application of GRC.

6.2.2 Formwork - The flexibility in shape and size, and the strongness even though of the thin sections make GRC a suitable material for casting permanent formwork. This formwork also improves the fire resisting quality.

6.2.3 Waffle pans - GRC waffle pans were used in the floor construction of a brewery building in London. They were 12.6 mm. thick and of 1.44 x 1.44 x 1.13 m. dimensions.

6.2.4 Pipes and pavements - Glass reinforced concrete pavement overlays 50 mm. and 75 mm. thick were used in St. Paul, Minnesota by using 1.36 percent by volume of alkali-resistant fibers. The composite concrete pipes have also been fabricated commercially by ARC concrete, near Bristol, England.

6.2.5 Linings and surface coatings - GRC was also used for lining sewer segments by the Greater London Council in a 1.75m diameter sewer below the Portobello Road. Surface coatings of E-glass fiber reinforced ordinary Portland cement were used in building blockwork walls in 1967 by the U. S. Department of Agriculture.

6.2.6 Marine applications - GRC has also found a place in the field of marine applications. The floating marine pontoon units were used on Lake Siljan in Sweden. Sheetpiling has been developed by Charcon Ringvaart of Holland for use in canal revetments. Boat hulls made out of two 10 mm. thick skins separated by a rigid foam core are also in use.

6.2.7 Miscellaneous - Various miscellaneous small units manufactured from GRC are in use. This includes shell units, small water tanks, swimming pools, low cost refugee housing, grain silos, manhole covers, ducting, road and garden furniture, window frames, fence posts, pallets, noise barriers and several other similar applications.

6.3 Economics

In the manufacture of GRC, the cost of the alkali-resistant fiber is relatively high. The hand spray process demands skilled labor, and a capital investment required for this kind of hand spray unit is approximately $10,000 (1977 estimate)(5). Whereas the sufficient product volume and standardization may be favorable for an automated spray-dewatering plant. The simplest automatic spray-dewatering plant requires the capital investment of approximately $70,000 (1977 estimate)(5).

This data proves that GRC cannot be considered as a cheap building material. Economically priced GRC can only be manufactured with well trained efficient operators who have well organized plants. The basic raw material cost for GRC can be roughly approximated to be around $4 to $5 per square meter for a composite with 5 percent glass fiber and 9.5 mm. thick without considering any wastage of materials (1977 estimate). The price of the finished product is affected by several factors like labor, production volume, mold cost, method of manufacture, overhead, etc. As a rough approximation, the architectural custom-made GRC panels may have the price range from $27 to $87 per square meter (1977 estimate)(5).

However, considering the total cost of a project, GRC may provide cost savings because of the following plus points.

(a) Comparative light weight provides cost savings in transportation and handling.

(b) High insulation values with thin wall panels provide more usable floor space.

(c) Because of the commendable fire resistance extra fire preventing measures may not be necessary.

(d) Flexibility in shape and size reduces the installation cost.

(e) No extra precision in handling and erection is required because of high impact strength.

(f) In most of the cases, surfaces are maintenance free.

The recent energy crisis also requires that the economy be related to the energy consumption of the products under consideration. From the obtained data it can be concluded that 1 Kg. of concrete requires approximately 9714 KJ, whereas 1 Kg. of GRC asks for 16210 KJ. However,

a typical GRC panel being 1/6 in weight as compared to a typical concrete panel, the energy consumption per square meter of panel area is much less in case of GRC panel. A reinforced concrete panel with the weight 225 Kg/m^2 consumes 2134021 KJ per square meter, whereas a GRC panel weighing 34 Kg per m^2 consumes 553928 KJ per square meter. It is obvious that, even considering energy criterion, GRC may prove to be an efficient material (5).

Chapter 7

CONCLUSION AND FURTHER RESEARCH RECOMMENDATIONS

7.1 Conclusion

Glass fiber reinforced cement made from alkali-resistant glass fiber is a promising new construction material. Even though it is a newborn technology in North America, it has been extensively used in Europe for the last eight years. A wide range of flexibility in properties can be achieved by varying the glass content and length, cement matrix and the method of fabrication.

The various advantages that can be derived from the application of GRC are the improvement in flexural strength, tensile strength, impact strength, fire resistance, insulation characteristics, flexibility in shape and size, maintenance free surface finish and comparatively light weight products. All these plus points have made GRC an eminently suitable construction material. Economics associated with the GRC manufacture are a little controversial.

When we consider the advantages of GRC, we should not forget technical limitations and the potential complications associated with it. Its field of application is merely confined to the non-structural components like cladding panels, partition walls, formwork, small containers, lining and coating material, etc. Further long term data are required to predict the behavior of GRC under the continuously subjected stress systems. Relatively high drying shrinkage is expected because generally no coarse aggregates are used. The temptation to use steel reinforcement along with GRC should be avoided because severe distortion and probably cracking may take place because of the relatively high

shrinkage. Strict quality control should be enforced and frequent testing of the test coupons cut from the cast boards should be carried out.

Extensive research is still in progress regarding the age effect on GRC composites. There are three major areas where further advances can be confidently predicted:

(i) Material and product specifications and codes of practice.

(ii) Automation of production processes.

(iii) Increased use in structural areas of applications.

7.2 Further Research Recommendations

Further research is recommended in order to break the barrier between non-structural and structural fields of applications. Satisfactory analysis and design procedures should be investigated to make GRC popular among the engineers as a structural material.

APPENDIX A

ABBREVIATIONS

GRC - Glass Fiber Reinforced Composite

RHS - Right Hand Side

MOR - Modulus of Rupture

CG - Center of Gravity

NA - Neutral Axis

UTS - Ultimate Tensile Strength

LOP - Limit of Proportionality

RH - Relative Humidity

pfa - pulverized fuel ash

BIBLIOGRAPHY

1. Hannant, D. J, "Fiber Cement and Fiber Concrete." A Wiley Interscience Publication.

2. Rilem Symposium, 1975, "Fiber Reinforced Cement and Concrete.

3. Jones, John and Thomas P. Lutz, "Glass Fiber Reinforced Concrete Products - Properties and Applications." PCI Journal/May-June, 1977, pp. 81-103.

4. Ali, M. A., A. J. Majumdar, and B. Singh, "Properties of Glass Fiber Cement - The Effect of Fiber Length and Content." Journal of Materials Science/10(1975), pp. 1732-1740.

5. Anand, Yogindra and Authors, "Reader Comments on Glass Fiber Reinforced Concrete Products - Properties and Applications by Jones, John, Lutz, Thomas P., PCI Journal/March-April 1978, pp. 106-107.

6. Majumdar, A. J. and V. Laws, "Fiber Cement Composites - Research at BRE." Composites/January 1979, pp. 17-27.

7. ACI Committee 544, "State-of-the-Art Report on Fiber Reinforced Concrete," ACI Journal/November 1973, pp. 729-744.

8. Cahn, David S., Craig J. Phillips, Ori Ishai, and Samual Aroni, "Durability of Fiber-glass Portland Cement Composites." ACI Journal/ March 1973, pp. 187-189.

9. Blackman, L.C.F., "Glass Fiber Reinforced Cement - A Progress Report." Composites/April 1979, pp. 69-72.

10. Majumdar, A. J., and R. W. Nurse, "Glass Fiber Reinforced Cement." Material Science and Engineering/August-September 1974, pp. 107-126.

11. Allen, H. G., "Glass-fiber Reinforced Cement, Strength and Stiffness," CIRIA Report 55, September 1975.

12. Laws, V., "The Efficiency of Fibrous Reinforcement of Brittle Matrices," Journal Physics D: Applied Physics, 4, 1737-1746 (1971)

13. Oakley, D. R. and B. A. Proctor, "Tensile Stress-Strain Behavior of Glass-fiber Reinforced Cement Composites," Fiber Reinforced Cement and Concrete, RILEM Symposium, 1975, pp. 347-359.

14. Aveston, J., R. A. Mercer, and J. M. Sillwood, "Fiber Reinforced Cements - Scientific Foundations for Specifications," Composites - Standards, Testing and Design, National Physical Laboratory Conference Proceedings, April 1974, pp. 93-103.

15. Cohen, E. B. and S. Diamond, "Validity of Flexural Strength Reduction as an Indication of Alkali Attack on Glass in Fiber Reinforced Cement Composites," Fiber Reinforced Cement and Concrete, RILEM Symposium, 1975, pp. 315-325.

ACKNOWLEDGMENTS

I extend my sincere appreciation to Dr. Stuart E. Swartz for his continuous guidance and assistance throughout my graduate program. I also express my appreciation to all of my examination committee members for their direct or indirect assistance in achieving my goal. I would like to thank Peggy Selvidge for deciphering my writing and preparing the final transcript.

MECHANICAL PROPERTIES OF GLASS FIBER REINFORCED CONCRETE AND APPLICATIONS IN STRUCTURAL DESIGN

by

Bakul B. Desai

B.E., L.D. College of Engineering
Gujarat University, 1977

AN ABSTRACT OF A MASTER'S REPORT

submitted in partial fulfillment of

the requirements for the degree

MASTER OF SCIENCE

Department of Civil Engineering

KANSAS STATE UNIVERSITY
Manhattan, Kansas

1980

ABSTRACT

Even though glass fiber reinforced composite is just at the initial stage of its development in North America, the booming trend toward its commercial development in Europe, the size of construction markets worldwide and a declining tendency in use of asbestos cement could make it the largest group of all fiber reinforced composite systems in the foreseeable future. This report mainly includes the history and development, the simplified theories of fiber reinforcement and their application to an analysis example. Also the mechanical behavior based on experimental testing, advantages, economics and some potential limitations associated with glass fiber reinforced composites are presented. The favorable modifications in various mechanical properties and some other properties governed by economical considerations provide the steps by which the glass fiber composites may climb the stairs to commercial welcome. However, the lack of detailed understanding in the behavior of such composites under sustained loading restricts the field of application to non-structural or semi-structural type. Research efforts, including those depicted in this report, are still in progress. It is quite likely that one day glass fiber composites may prove to be the most suitable construction material.